cleus-to-cytoplasm transport of HIV-1 mRNA, and HIV-1 particle assembly, since HIV-1 does not encode own RNA helicase [15,17]. Indeed, DDX1 and DDX3 have been implicated in post-transcriptional regulation of HIV-1 [18–22]. Both DDX1 and DDX3 interact with HIV-1 Rev and enhance the Rev-dependent HIV-1 nuclear export [18–22]. In addition to DDX1 and DDX3, we have demonstrated that DDX5, DDX17, DDX21, and DDX56, interacted with Rev and stimulated the Rev function (Figs. 1 and 2). Quite recently, Naji et al. employed the proteomics and statistical analysis to identify candidate host cell factors that interact with Rev/RRE [25]. In addition to above DDX RNA helicases, they also identified DHX36, DDX24, DHX9, and DDX47 as the Rev-binding DEAD/H-box proteins [25]. Their interactome analysis of HIV-1 Rev supports and compensates our and their primary findings each other, since they did not demonstrate the direct evidence of these DDX RNA helicases modulate on the Rev function as well as their subcellular localization.

Lorgeoux et al. proposed that DDX1 and DDX3 act sequentially in the Rev-dependent RNA export [17]. DDX1 first binds to Rev and promotes Rev oligomerization on the RRE RNA. Then, the oligomerized Rev recruits the CRM1/DDX3 complex that subsequently exports the RRE-containing HIV-1 RNA into the cytoplasm. Accordingly, we have found that combination of DDX1 and DDX3 cooperated to synergistically enhance the Rev-dependent nuclear export function (Fig. 4). We have demonstrated an interaction of DDX3 with DDX5 (Fig. 3), indicating the cross-talk among distinct DDX RNA helicases. In this context, other combinations of distinct DDX RNA helicases, such as DDX3 and DDX5 or DDX1 and DDX21, synergistically cooperated to stimulate the HIV-1 Rev function (Fig. 4). In addition to DDX, RHA also plays a role in Rev/RRE-dependent post-transcriptional regulation of HIV-1 [26]. RHA binds weakly to HIV-1 RRE independently of Rev. Thus, various RNA helicases seemed to be involved in the post-transcriptional regulation of HIV-1, however, it remains to be clarified when and where these distinct RNA helicases sequentially or hierarchically orchestrate the Rev-dependent RNA export.

Although we failed to observe the prominent effect of DDX6 on the HIV-1 Rev function (Fig. 1), DDX6 was reported to affect the viral genome packaging of foamy virus, a spumaretrovirus [27]. Relocation of DDX6 from P-bodies and stress granules to virus assembly sites at the perinuclear region was seen in foamy virus infected cells. However, DDX6 did not interact with Gag proteins and was not incorporated into the virion. In contrast, Reed et al. recently reported that DDX6 and Ago2 bind to HIV-1 Gag and DDX6 facilitates Gag assembly independent of HIV-1 RNA packaging [28]. Notably, DDX6 and Ago2, that are major components of P-body and act as microRNA effectors, suppress the HIV-1 replication [29,30].

Finally, Van't Wout et al. and Krishnan and Zeichner reported that the expression of several DDX RNA helicases, including DDX10, DDX18, DDX21, DDX23, DDX39, and DDX52 is modulated during HIV-1 infection [31–33]. Intriguingly, several DDX RNA helicases were upregulated during HIV-1 infection from latency toreactivation [33], however, the biological significance of these phenomenon was not understood. Altogether, several distinct DDX DEAD-box RNA helicases could cross-talk and contribute to the HIV-1 life cycle at multiple stages.

Acknowledgments

We thank Drs. Didier Trono, Kuan-Teh Jeang, Venkat S. Yedavalli, Roger J. Pomerantz, and Jianhua Fang for pcRev, pHA-DDX3, and pDM628, respectively. This work was supported by a Grant-in-Aid for Scientific Research (C) from the Japan Society for the Promotion of Science (JSPS), by a Grant-in-Aid for Research on Hepatitis from the Ministry of Health, Labor, and Welfare of Japan, by the Imai Memorial Trust for AIDS Research, by the Naito Foundation, and by the Mochida Memorial Foundation for Medical and Pharmaceutical Research. M. K. was supported by a Research Fellowship from JSPS for Young Scientists.

References

[1] K.T. Jeang, H. Xiao, E.A. Rich, Multifaceted activities of the HIV-1 transactivator of transcription, Tat, J. Biol. Chem. 274 (1999) 28837–28840.
[2] B. Berkhout, R.H. Silverman, K.T. Jeang, Tat *trans*-activates the human immunodeficiency virus through a nascent RNA target, Cell 59 (1989) 273–282.
[3] T.J. Hope, R.J. Pomerantz, The human immunodeficiency virus type 1 Rev protein: a pivotal protein in the viral life cycle, Curr. Top. Microbiol. Immunol. 193 (1995) 91–105.
[4] V.W. Pollard, M.H. Malim, The HIV-1 Rev protein, Annu. Rev. Microbiol. 52 (1998) 491–532.
[5] B.R. Cullen, Nuclear mRNA export: insights from virology, Trends Biochem. Sci. 28 (2003) 419–424.
[6] D. Trono, D. Baltimore, A human cell factor is essential for HIV-1 Rev action, EMBO J. 9 (1990) 4155–4160.
[7] S. Rocak, P. Linder, DEAD-box proteins: the driving forces behind RNA metabolism, Nat. Rev. Mol. Cell Biol. 5 (2004) 232–241.
[8] E.A. Gustafson, G.M. Wessel, DEAD-box helicases: posttranslational regulation and function, Biochem. Biophys. Res. Commun. 395 (2010) 1–6.
[9] Y. Ariumi, M. Kuroki, K. Abe, et al., DDX3 DEAD-box RNA helicase is required for hepatitis C virus RNA replication, J. Virol. 81 (2007) 13922–13926.
[10] Y. Ariumi, M. Kuroki, Y. Kushima, et al., Hepatitis C virus hijacks P-body and stress granule components around lipid droplets, J. Virol. 85 (2011) 6882–6892.
[11] P.Y. Goh, Y.J. Tan, S.P. Lim, et al., Cellular RNA helicase p68 relocalization and interaction with the hepatitis C virus (HCV) NS5B protein and the potential role of p68 in HCV RNA replication, J. Virol. 78 (2004) 5288–5298.
[12] M. Kuroki, Y. Ariumi, M. Hijikata, et al., PML tumor suppressor protein is required for HCV production, Biochem. Biophys. Res. Commun. 430 (2013) 592–597.
[13] Y. Watanabe, N. Ohtaki, Y. Hayashi, et al., Autogenous translational regulation of the Borna disease virus nagative control factor X from polycistronic mRNA using host RNA helicases, PLoS Pathog. 5 (2009) e1000654.
[14] Z. Xu, R. Anderson, T.C. Hobman, The capsid-binding nucleolar helicase DDX56 is important for infectivity of West Nile virus, J. Virol. 85 (2011) 5571–5580.
[15] A.D. Kwong, B.G. Rao, K.T. Jeang, Viral and cellular RNA helicases as antiviral targets, Nat. Rev. Drug Discov. 4 (2005) 845–853.
[16] A. Utama, H. Shimizu, F. Hasebe, et al., Role of the DExH motif of the Japanese encephalitis virus and hepatitis C virus NS3 proteins in the ATPase and RNA helicase activities, Virology 273 (2000) 316–324.
[17] R.P. Lorgeoux, F. Guo, C. Liang, From promoting to inhibiting: diverse roles of helicases in HIV-1 replication, Retrovirology 9 (2012) 79.
[18] V.S. Yedavalli, C. Neuveut, Y.H. Chi, et al., Requirement of DDX3 DEAD box RNA helicase for HIV-1 Rev-RRE export function, Cell 119 (2004) 381–392.
[19] J. Fang, S. Kubota, B. Yang, et al., A DEAD box protein facilitates HIV-1 replication as a cellular co-factor of Rev, Virology 330 (2004) 471–480.
[20] J. Fang, E. Acheampong, R. Dave, et al., The RNA helicase DDX1 is involved in restricted HIV-1 Rev function in human astrocytes, Virology 336 (2005) 299–307.
[21] R.M. Robertson-Anderson, J. Wang, S.P. Edgcomb, et al., Single-molecule studies reveal that DEAD box protein DDX1 promotes oligomerization of HIV-1 Rev on the Rev response element, J. Mol. Biol. 410 (2011) 959–971.
[22] S.P. Edgcomb, A.B. Carmel, S. Naji, et al., DDX1 is an RNA-denpendent ATPase involved in HIV-1 Rev function and virus replication, J. Mol. Biol. 415 (2012) 61–74.
[23] Y. Ariumi, A. Kaida, M. Hatanaka, et al., Functional cross-talk of HIV-1 Tat with p53 through its C-terminal domain, Biochem. Biophys. Res. Commun. 287 (2001) 556–561.
[24] Y. Ariumi, D. Trono, Ataxia-telangiectasia-mutated (ATM) protein can enhance human immunodeficiency virus type 1 replication by stimulating Rev function, J. Virol. 80 (2006) 2445–2452.
[25] S. Naji, G. Ambrus, P. Cimermancic, et al., Host cell interactome of HIV-1 Rev includes RNA helicases involved in multiple facets of virus production, Mol. Cell. Proteomics 11 (2012) M111.
[26] J. Li, H. Tang, T.M. Mullen, et al., A role for RNA helicase A in post-transcriptional regulation of HIV type 1, Proc. Natl. Acad. Sci. USA 96 (1999) 709–714.
[27] S.F. Yu, P. Lujan, D.L. Jackson, et al., The DEAD-box RNA helicase DDX6 is required for efficient encapsidation of a retroviral genome, PLoS Pathog. 7 (2011) e1002303.
[28] J.C. Reed, B. Molter, C.D. Geary, et al., HIV-1 Gag co-opts a cellular complex containing DDX6, a helicase that facilitates capsid assembly, J. Cell Biol. 198 (2012) 439–456.
[29] R. Nathans, C.Y. Chu, A.K. Serquina, et al., Cellular microRNA and P bodies modulate host-HIV-1 interactions, Mol. Cell 34 (2009) 696–709.
[30] C. Chable-Bessia, O. Meziane, D. Latreille, et al., Suppression of HIV-1 replication by microRNA effectors, Retrovirology 6 (2009) 26.

[31] A.B. Van't Wout, G.K. Lehrman, S.A. Mikheeva, et al., Cellular gene expression upon human immunodeficiency virus type 1 infection of $CD4^+$-T-cell lines, J. Virol. 77 (2003) 1392–1402.

[32] V. Krishnan, S.L. Zeichner, Alterations in the expression of DEAD-box and other RNA binding proteins during HIV-1 replication, Retrovirology 1 (2004) 42.

[33] V. Krishnan, S.L. Zeichner, Host cell gene expression during human immunodeficiency virus type 1 latency and reactivation and effects of targeting genes that are differentially expressed in viral latency, J. Virol. 78 (2004) 9458–9473.

Biochemical and Biophysical Research Communications 441 (2013) 607–611

Contents lists available at ScienceDirect

Biochemical and Biophysical Research Communications

journal homepage: www.elsevier.com/locate/ybbrc

DDX3 RNA helicase is required for HIV-1 Tat function

Mariko Yasuda-Inoue, Misao Kuroki, Yasuo Ariumi *

Center for AIDS Research, Kumamoto University, Kumamoto 860-0811, Japan

ARTICLE INFO

Article history:
Received 1 October 2013
Available online 30 October 2013

Keywords:
HIV-1
Tat
DDX3
Stress granule
P-body

ABSTRACT

Host RNA helicase has been involved in human immunodeficiency virus type 1 (HIV-1) replication, since HIV-1 does not encode an RNA helicase. Indeed, DDX1 and DDX3 DEAD-box RNA helicases are known to be required for efficient HIV-1 Rev-dependent RNA export. However, it remains unclear whether DDX RNA helicases modulate the HIV-1 Tat function. In this study, we demonstrate, for the first time, that DDX3 is required for the HIV-1 Tat function. Notably, DDX3 colocalized and interacted with HIV-1 Tat in cytoplasmic foci. Indeed, DDX3 localized in the cytoplasmic foci P-bodies or stress granules under stress condition after the treatment with arsenite. Importantly, only DDX3 enhanced the Tat function, while various distinct DEAD-box RNA helicases including DDX1, DDX3, DDX5, DDX17, DDX21, and DDX56, stimulated the HIV-1 Rev-dependent RNA export function, indicating a specific role of DDX3 in Tat function. Indeed, the ATPase-dependent RNA helicase activity of DDX3 seemed to be required for the Tat function as well as the colocalization with Tat. Furthermore, the combination of DDX3 with other distinct DDX RNA helicases cooperated to stimulate the Rev but not Tat function. Thus, DDX3 seems to interact with the HIV-1 Tat and facilitate the Tat function.

1. Introduction

The gene expression of human immunodeficiency virus type 1 (HIV-1) is regulated transcriptionally by Tat through its binding to a nascent viral *trans*-activation responsive (TAR) RNA [1,2], and post-transcriptionally by Rev through its association with Rev-responsive element (RRE) RNA in the *env* gene [3–5]. Tat binds to TAR RNA and recruits transcription factors, such as p300/CREB-binding protein (CBP), p300/CBP-associated factor (PCAF), chromatin remodeling factors Brahma (BRM), Brahma-related gene 1 (BRG1), integrase interactor 1 (INI1), and positive transcription elongation factor (P-TEFb), a complex of cyclin T1 and cyclin-dependent kinase 9 (CDK9), to stimulate both transcription initiation from the HIV-1 long terminal repeat (LTR) and transcription elongation [1,2,6,7]. CDK9 hyperphosphorylates the C-terminal domain (CTD) of RNA polymerase II and activates transcription elongation.

DEAD-box RNA helicases are involved in various RNA metabolic processes, including transcription, translation, RNA splicing, RNA transport, and RNA degradation in the ATPase-dependent manner [8–10]. Host RNA helicases may be involved in HIV-1 replication [11,12], since HIV-1 does not encode an RNA helicase. In fact, DDX1 and DDX3 have been implicated in the replication of HIV-1 replication [13–15]. Both DDX1 and DDX3 interact with HIV-1 Rev and enhance Rev-dependent HIV-1 nuclear export [13–15]. In addition, we recently demonstrated that several DDX, including DDX1, DDX3, DDX5, DDX17, DDX21, and DDX56 interact with HIV-1 Rev and enhance the Rev-dependent nuclear export [16]. However, the role of these DDX DEAD-box RNA helicases in HIV-1 Tat function is still unknown. To address this issue, we first examined the interaction of these DDX RNA helicases with HIV-1 Tat and the potential role of DDX in the Tat function.

2. Material and methods

2.1. Cell culture

293FT cells were cultured in Dulbecco's modified Eagle's medium (DMEM; Invitrogen, Carlsbad, CA, USA) supplemented with 10% fetal bovine serum (FBS).

2.2. Plasmids

We used pcDNA3-HA, pcDNA3-FLAG, pHLV-1-LTR-Luc [17], pHA-DDX3 [13,18,19], pcRev, pDM628 [14,15,20], pcDNA3-Tat101-FLAG [21], pcDNA3-HA-DDX1, pcDNA3-HA-DDX5, pcDNA3-HA-DDX17, pcDNA3-HA-DDX21, and pcDNA3-HA-DDX56 [16].

---

* Corresponding author. Address: Center for AIDS Research, Kumamoto University, 2-2-1 Honjo, Chuo-ku, Kumamoto 860-0811, Japan. Fax: +81 96 373 6834.
E-mail address: ariumi@kumamoto-u.ac.jp (Y. Ariumi).

0006-291X/$ - see front matter © 2013 Elsevier Inc. All rights reserved.
http://dx.doi.org/10.1016/j.bbrc.2013.10.107

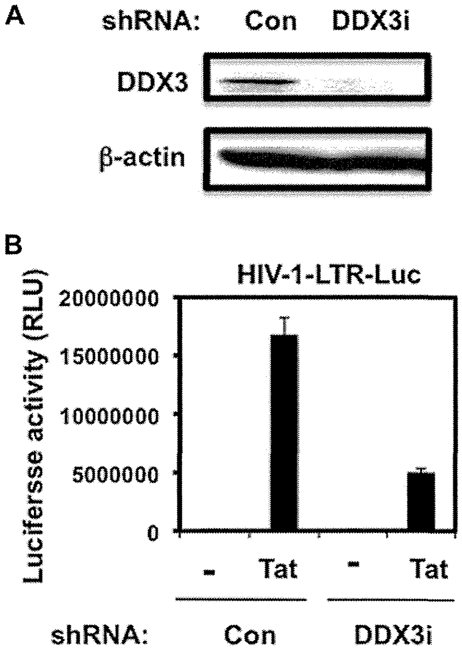

Fig. 1. Requirement of DDX3 for HIV-1 Tat function. (A) Inhibition of DDX3 expression by shRNA-producing lentiviral vector. The results of Western blot analysis of cellular lysates with anti-DDX3 or anti-β-actin antibody in the cells expressing shRNA targeted to DDX3 (DDX3i) as well as in the cells transduced with a control lentiviral vector (shCon) are shown. (B) HIV-1 Tat-mediated transcription in the DDX3 knockdown cells. Cells (2×10^4 cells) were cotransfected with pHIV-1-LTR-Luc [7,17,20] (100 ng) and/or pcDNA3-Tat101-FLAG [21] (100 ng). 24 h after transfection, luciferase activity in the cellular lysates was measured. Results are from three independent experiments.

2.3. Lentiviral vector production

pLV-DDX3i and the vesicular stomatitis virus (VSV)-G-pseudotyped HIV-1-based vector system has been described previously [18,22,23]. The lentiviral vector particles were produced by transient transfection of the second-generation packaging construct pCMV-ΔR8.91 [22,23] and the VSV-G-envelope-expressing plasmid pMDG2 as well as pRDI292 into 293FT cells with FuGENE 6 (Promega, Madison, WI, USA).

2.4. Luciferase assay

Plasmids were transfected into 293FT cells (2×10^4 cells) using the FuGENE 6 transfection reagent. Luciferase assays were performed 24 h after transfection using luciferase assay reagent according to the manufacturer's instructions (Promega). All transfections utilized equal total amounts of plasmid DNA quantities owing to the addition of empty vector into the transfection mixture. Results were obtained through three independent transfections. A lumat LB9507 luminometer (Berthold, Bad Wildbad, Germany) was used to detect the luciferase activity.

2.5. Western blot analysis

Cells were lysed in buffer containing 50 mM Tris–HCl (pH 8.0), 150 mM NaCl, 4 mM EDTA, 1% Nonidet P (NP)-40, 0.1% sodium dodecyl sulfate (SDS), 1 mM dithiothreitol (DTT) and 1 mM phenylmethylsulfonyl fluoride (PMSF). Supernatants from these lysates were subjected to SDS-polyacrylamide gel electrophoresis, followed by immunoblot analysis using anti-HA (HA-7; Sigma, Saint Louis, MI, USA), anti-DDX3 (54257 [NT] and 5428 [IN]; Anaspec, San Jose, CA, USA), anti-DDX5 (A300-523A; Bethyl Laboratories, Montgomery, TX, USA) anti-β-actin (A5441, Sigma), or anti-FLAG antibody (M2, Sigma).

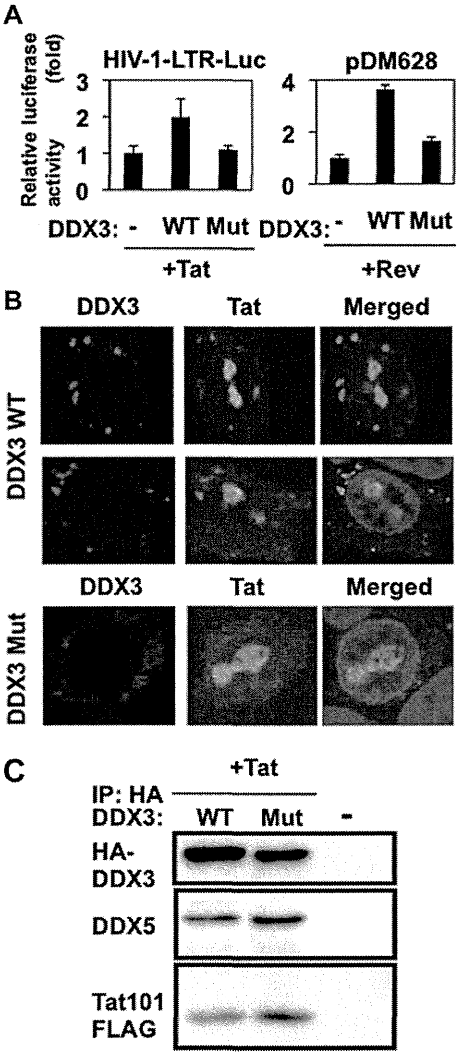

Fig. 2. DDX3 interacts with HIV-1 Tat in cytoplasmic foci. (A) The ATPase-dependent RNA helicase activity of DDX3 is required for the Tat function. 293FT cells (2×10^4 cells) were cotransfected with pHIV-1-LTR-Luc (100 ng), pHA-DDX3 WT (wild-type) or pHA-DDX3 Mut (ATPase-defective mutant) [13], and/or pcDNA3-Tat101-FLAG (100 ng). 24 h after transfection, luciferase activity in the cellular lysates was measured. (B) DDX3 colocalizes with Tat. 293FT cells cotransfected with pHA-DDX3 WT or pHA-DDX3 Mut (200 ng) and pcDNA3-Tat101-FLAG (200 ng) were examined by confocal laser scanning microscopy. Cells were stained with anti-DDX3 (LS-C64576) and Cy3-conjugated anti-mouse IgG antibody followed by staining with FITC-conjugated anti-FLAG antibody, and then visualized with Cy3 (DDX3) or FITC (Tat). Nuclei were stained with DAPI. Images were visualized by using confocal laser scanning microscopy. The right panels exhibit the two-color overlay images (Merged). (C) 293FT cells were cotransfected with pcDNA3-Tat101-FLAG (2 μg) and either pHA-DDX3 WT or pHA-DDX3 Mut (2 μg). The cell lysates were immunoprecipitated with an anti-HA antibody, followed by immunoblot analysis using anti-HA, anti-DDX5, or anti-FLAG antibody. (For interpretation of the references to color in this figure legend, the reader is referred to the web version of this article.)

2.6. Immunoprecipitation

Cells were lysed in buffer containing 10 mM Tris–HCl (pH 8.0), 150 mM NaCl, 4 mM EDTA, 0.1% NP-40, 10 mM NaF, 1 mM DTT and 1 mM PMSF. Lysates were pre-cleared with 30 μl of protein-G-Sepharose (GE Healthcare Bio-Sciences, Uppsala, Sweden). Pre-cleared supernatants were incubated with 5 μg of anti-HA

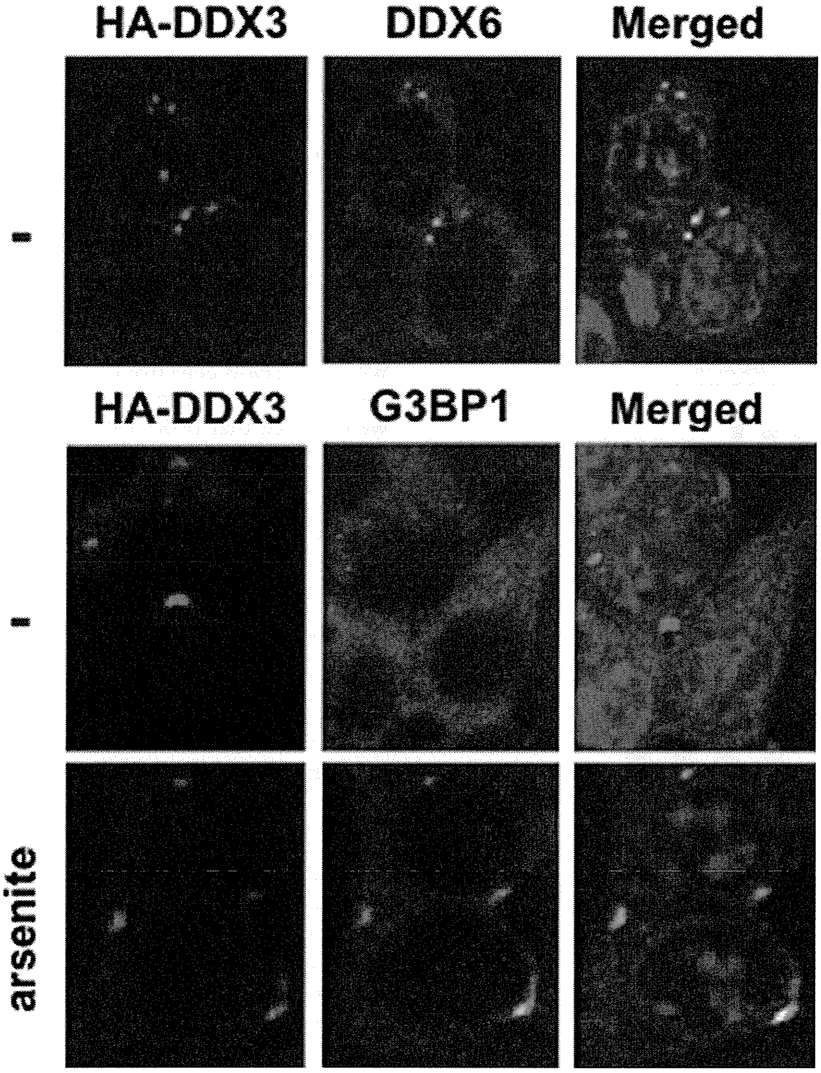

Fig. 3. DDX3 localizes in P-bodies and stress granules. 293FT cells expressing HA-DDX3 were treated with or without 0.5 mM arsenite for 45 min. Cells were stained with anti-HA and anti-DDX6, or anti-G3BP1 antibodies and were examined by confocal laser scanning microscopy. Nuclei were stained with DAPI.

antibody (3F10; Roche Diagnostics, Mannheim, Germany) at 4 °C for 1 h. Following absorption of the precipitates on 30 μl of protein-G-Sepharose resin for 1 h, the resin was washed four times with 700 μl lysis buffer. Proteins were eluted by boiling the resin for 5 min in 2× Laemmli sample buffer. The proteins were then subjected to SDS–PAGE, followed by immunoblotting analysis using anti-HA, anti-DDX5, or anti-FLAG antibody.

2.7. Immunofluorescence and confocal microscopic analysis

Cells were fixed in 3.6% formaldehyde in phosphate-buffered saline (PBS), permeabilized in 0.1% Nonidet P-40 in PBS at room temperature, and incubated with anti-HA (HA-7; Sigma), anti-DDX6 (A300-460A; Bethyl), anti-DDX3X (LS-C64576; LifeSpan BioSciences, Seattle, WA, USA), and/or anti-FLAG (M2) antibody at a 1:300 dilution in PBS containing 3% bovine serum albumin (BSA) at 37 °C for 30 min. They were then stained with Cy3-conjugated anti-mouse antibody and fluorescein isothiocyanate (FITC)-conjugated anti-rabbit antibody (Jackson ImmunoResearch, West Grove, PA, USA) at a 1:300 dilution in PBS containing BSA at 37 °C for 30 min. Nuclei were stained with DAPI (4′,6′-diamidino-2-phenylindole). Following extensive washing in PBS, the cells were mounted on slides using a mounting media of SlowFade Gold antifade reagent (Invitrogen) added to reduce fading. Samples were viewed under a confocal laser-scanning microscope (FV1000; Olympus, Tokyo, Japan).

3. Results

3.1. DDX3 facilitates HIV-1 Tat function

DDX3 DEAD-box RNA helicase is known to be required for efficient HIV-1 Rev-dependent RNA export [13]. However, it remains unclear whether DDX3 modulates the HIV-1 Tat function. To address this issue, we first used lentivirus vector-mediated RNA interference to stably knockdown DDX3. To express shRNA targeted to DDX3, we used a VSV-G-pseudotyped HIV-1-based vector system [22,23]. Western blot analysis of the lysates demonstrated very effective knockdown of DDX3 (Fig. 1A). In this context, the Tat-induced transcription from the HIV-1-long terminal repeat (LTR) within a transfected LTR-luciferase reporter plasmid [7,17,20] was significantly impaired to compared the control cells (Fig. 1B), suggesting that DDX3 is required for the Tat function. Reciprocally, overexpression of DDX3 enhanced the Tat-induced transcription as well as the Rev-dependent nuclear export function (Fig. 2A). Thus, DDX3 seems to facilitate the Tat function.

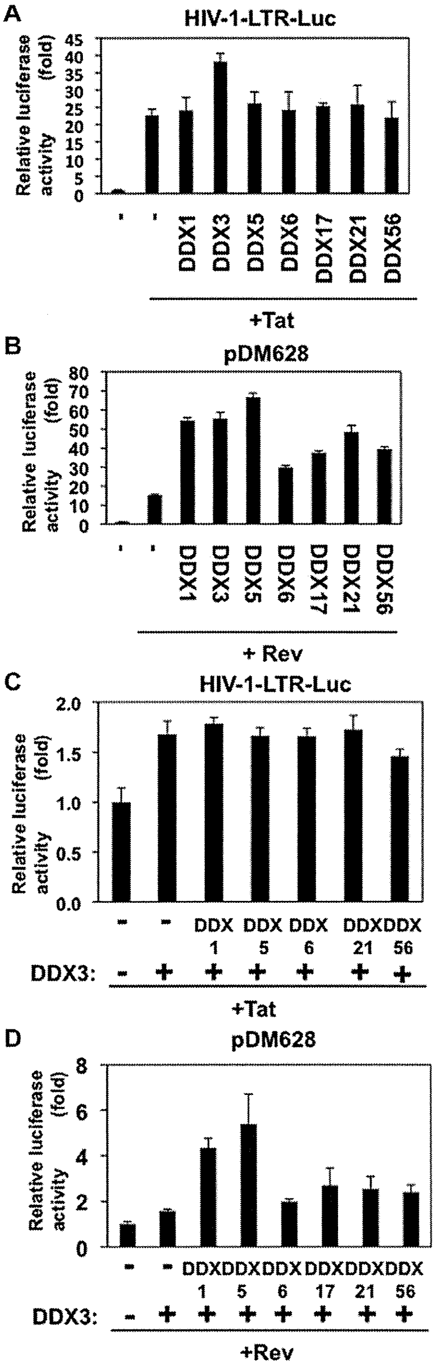

Fig. 4. Combination of distinct DDX RNA helicases cooperate to enhance the Rev but not the Tat function. (A) 293FT cells (2×10^4 cells) were cotransfected with pHIV-1-LTR-Luc (100 ng), pcDNA3-HA-DDX1, pHA-DDX3, pcDNA3-HA-DDX5, pcDNA3-HA-DDX6, pcDNA3-HA-DDX17, pcDNA3-HA-DDX21, or pcDNA3-HA-DDX56 (100 ng) [16], and/or pcDNA3-Tat101-FLAG (100 ng). 24 h after transfection, luciferase activity in the cellular lysates was measured. Results are from three independent experiments. (B) 293FT cells (2×10^4 cells) were cotransfected with pDM628 (100 ng), pcDNA3-HA-DDX1, pHA-DDX3, pcDNA3-HA-DDX5, pcDNA3-HA-DDX6, pcDNA3-HA-DDX17, pcDNA3-HA-DDX21, or pcDNA3-HA-DDX56 (100 ng), and/or pcRev (100 ng). 24 h after transfection, luciferase activity in the cellular lysates was measured. (C) 293FT cells (2×10^4 cells) were cotransfected with pHIV-1-LTR-Luc (100 ng), pcDNA3-Tat101-FLAG (100 ng), pHA-DDX3 (100 ng), and/or pcDNA3-HA-DDX1, pcDNA3-HA-DDX5, pcDNA3-HA-DDX6, pcDNA3-HA-DDX21, or pcDNA3-HA-DDX56 (100 ng). 24 h after transfection, luciferase activity in the cellular lysates was measured. (D) 293FT cells (2×10^4 cells) were cotransfected with pDM628 (100 ng), pcRev (100 ng), pHA-DDX3, and/or pHA-DDX1, pcDNA3-HA-DDX5, pcDNA3-HA-DDX6, pcDNA3-HA-DDX17, pcDNA3-HA-DDX21, or pcDNA3-HA-DDX56 (100 ng). 24 h after transfection, luciferase activity in the cellular lysates was measured.

3.2. DDX3 colocalized and interacted with HIV-1 Tat in cytoplasmic foci

To clarify the mechanism how DDX3 enhances the Tat function, we used an ATPase-defective mutant of DDX3 (Mut) [13]. Consequently, this mutant of DDX3 did not enhance the Tat-induced transcription as well as the Rev-dependent nuclear export function (Fig. 2A). Since this ATPase-defective mutant of DDX3 is known to abolish DDX3's RNA-unwinding activity, the ATPase-dependent RNA helicase activity of DDX3 seemed to be required for both Tat and Rev function. Recently, DDX3 was reported to associate with stress granules in translational regulation [24]. Consistently, wild-type (WT) DDX3 colocalized with Tat in the cytoplasmic foci, whereas ATPase-defective mutant of DDX3 (Mut) was dispersed in the cytoplasm and it did not colocalize with Tat (Fig. 2B). In fact, we observed that DDX3 localized in P-bodies and stress granules (Fig. 3). Moreover, HA-DDX3 (both WT and Mut), endogenous DDX5, and Tat could be co-immunoprecipitated with anti-HA antibody by the immunoprecipitation analysis, indicating that DDX3 forms a complex with Tat and DDX5 whether directly or indirectly (Fig. 2C).

3.3. Combination of distinct DDX RNA helicases cooperate to enhance the Rev but not the Tat function

So far, several DDX RNA helicases have been implicated in the HIV-1 Rev function [13–16], while the role of DDX DEAD-box RNA helicases on the HIV-1 Tat function was not fully understood. Finally, we further investigated the potential role of other DDX DEAD-box RNA helicases on the Tat function. For this, we examined whether various DDX DEAD-box RNA helicases, including DDX1, DDX3, DDX5, DDX6, DDX17, DDX21, and DDX56, modulates Tat-mediated *trans*-activation function. Consequently, only DDX3 could facilitate the Tat-induced transcription (Fig. 4A). In contrast, other DDX RNA helicases did not affect the Tat-induced transcription, while all tested DDX could stimulate the Rev-dependent nuclear export function using the Rev-dependent luciferase-based reporter plasmid pDM628 [14,15,20] (Fig. 4A and B), indicating that DDX3 specifically modulates the Tat function. As well, we found that various combination series of DDX3 with other DDXs, including DDX1, DDX5, DDX6, DDX21, and DDX56, did not synergize to enhance the Tat function compared to that of DDX3 alone (Fig. 4C). Conversely, the combination of DDX3 with other DDXs could synergistically enhance the Rev function (Fig. 4D). Thus, DDX3 specifically enhanced the HIV-1 Tat function.

Altogether, DDX3 RNA helicases seemed to interact with HIV-1 Tat and modulated the Tat function.

4. Discussion

Host RNA helicases have been involved in HIV-1 mRNA transcription [11,12]. Indeed, the Werner syndrome helicase (WRN) and RNA helicase A (RHA) were reported to act as cofactors of Tat and enhance HIV-1 gene expression [25,26]. WRN, a member of the RecQ helicase family, participates in DNA replication, DNA recombination, double strand break repair, telomere maintenance, and p53 activation. Mutations of *wrn* gene cause the Werner syndrome (WS), an autosomal recessive premature aging disorder associated with cancer disposition. WRN also promotes RNA polymerase II-dependent transcription. Thus, WRN was recently shown to interact with HIV-1 Tat and promote HIV-1 LTR transactivation [25]. Indeed, WRN participates in the recruitment of PCAF/P-TEFb-containing transcription complex to HIV-1 LTR. In addition to WRN, RHA also promotes the TAR-dependent HIV-1 gene expression [26]. RHA increases both basal level transcription from

HIV-1 LTR and Tat-induced transcription. Furthermore, Cocude et al. reported that a novel DExH RNA helicase RH116 was found localized in the nucleus of HIV-1 infected cells and augmented the transcription of unspliced HIV-1 transcript [27], while it remains unclear whether RHA and RH116 directly interact with Tat and provide direct role of the Tat-induced transcription. On the other hand, we have demonstrated that DDX3 bound to Tat and modulated the Tat function (Figs. 1 and 2). Atleast, the ATPase-dependent RNA helicase activity of DDX3 was required for the modulation of Tat function (Fig. 2A). Accordingly, DDX3 was reported to associated with translational regulation through interaction with eIF4E/poly(A)-binding protein 1 (PABP1) in stress granules [24]. In fact, DDX3 WT but not DDX3 Mut colocalized with Tat in cytoplasmic foci (Fig. 2B) and DDX3 localized in stress granules (Fig. 3). In this regard, Soto-Rifo et al. recently reported that DDX3 associates with eIF4F complex through an eIF4G and PABP1 double interaction to promote translation initiation of HIV-1 genomic (g) RNA [28]. Similarly, RHA also enhances HIV-1 RNA translation [29] like DDX3. This function of RHA depends on its binding to the R-U5 sequence of HIV-1 RNA termed post-transcriptional control element (PCE). Thus, DDX3 seems to be involved in HIV-1 translation through an interaction with Tat and HIV-1 5′ untranslated region (UTR) in stress granules.

Acknowledgments

We thank Drs. Didier Trono, Kuan-Teh Jeang, Venkat S. Yedavalli, Roger J. Pomerantz, Jianhua Fang, Hiroyuki Sakai, Monsef Benkirane for pcRev, pHA-DDX3, pDM628, pHTLV-1-LTR-Luc, pcDNA3-Tat101-FLAG, respectively. This work was supported by a Grant-in-Aid for Scientific Research (C) from the Japan Society for the Promotion of Science (JSPS), by a Grant-in-Aid for Research on Hepatitis from the Ministry of Health, Labor, and Welfare of Japan, by the Imai Memorial Trust for AIDS Research, by the Naito Foundation, and by the Mochida Memorial Foundation for Medical and Pharmaceutical Research.

References

[1] K.T. Jeang, H. Xiao, E.A. Rich, Multifaceted activities of the HIV-1 transactivator of transcription, Tat, J. Biol. Chem. 274 (1999) 28837–28840.

[2] B. Berkhout, R.H. Silverman, K.T. Jeang, Tat *trans*-activates the human immunodeficiency virus through a nascent RNA target, Cell 59 (1989) 273–282.

[3] T.J. Hope, R.J. Pomerantz, The human immunodeficiency virus type 1 Rev protein: a pivotal protein in the viral life cycle, Curr. Top. Microbiol. Immunol. 193 (1995) 91–105.

[4] V.W. Pollard, M.H. Malim, The HIV-1 Rev protein, Annu. Rev. Microbiol. 52 (1998) 491–532.

[5] B.R. Cullen, Nuclear mRNA export: insights from virology, Trends Biochem. Sci. 28 (2003) 419–424.

[6] V.W. Gautier, L. Gu, N. O'Donoghue, et al., In vitro nuclear interactome of the HIV-1 Tat protein, Retrovirology 6 (2009) 47.

[7] Y. Ariumi, F. Serhan, P. Turelli, et al., The integrase interactor 1 (INI1) proteins facilitate Tat-mediated human immunodeficiency virus type 1 transcription, Retrovirology 3 (2006) 47.

[8] S. Rocak, P. Linder, DEAD-box proteins: the driving forces behind RNA metabolism, Nat. Rev. Mol. Cell Biol. 5 (2004) 232–241.

[9] O. Cordin, J. Banroques, K. Tanner, et al., The DEAD-box protein family of RNA helicases, Gene 367 (2006) 17–37.

[10] E. Jankowsky, RNA helicases at work: binding and rearranging, Trends Biochem. Sci. 36 (2010) 19–29.

[11] R.P. Lorgeoux, F. Guo, C. Liang, From promoting to inhibiting: diverse roles of helicases in HIV-1 replication, Retrovirology 9 (2012) 79.

[12] K.T. Jeang, V. Yedavalli, Role of RNA helicases in HIV-1 replication, Nucleic Acids Res. 34 (2006) 4198–4205.

[13] V.S. Yedavalli, C. Neuveut, Y.H. Chi, et al., Requirement of DDX3 DEAD box RNA helicase for HIV-1 Rev-RRE export function, Cell 119 (2004) 381–392.

[14] J. Fang, S. Kubota, B. Yang, et al., A DEAD box protein facilitates HIV-1 replication as a cellular co-factor of Rev, Virology 330 (2004) 471–480.

[15] J. Fang, E. Acheampong, R. Dave, et al., The RNA helicase DDX1 is involved in restricted HIV-1 Rev function in human astrocytes, Virology 336 (2005) 299–307.

[16] M. Yasuda-Inoue, M. Kuroki, Y. Ariumi, Distinct DDX DEAD-box RNA helicases cooperate to modulate the HIV-1 Rev function, Biochem. Biophys. Res. Commun. 434 (2013) 803–808.

[17] Y. Ariumi, A. Kaida, M. Hatanaka, et al., Functional cross-talk of HIV-1 Tat with p53 through its C-terminal domain, Biochem. Biophys. Res. Commun. 287 (2001) 556–561.

[18] Y. Ariumi, M. Kuroki, K. Abe, et al., DDX3 DEAD-box RNA helicase is required for hepatitis C virus RNA replication, J. Virol. 81 (2007) 13922–13926.

[19] Y. Ariumi, M. Kuroki, Y. Kushima, et al., Hepatitis C virus hijacks P-body and stress granule components around lipid droplets, J. Virol. 85 (2011) 6882–6892.

[20] Y. Ariumi, D. Trono, Ataxia-telangiectasia-mutated (ATM) protein can enhance human immunodeficiency virus type 1 replication by stimulating Rev function, J. Virol. 80 (2006) 2445–2452.

[21] V. Brès, R.E. Kiernan, L.K. Linares, et al., A non-proteolytic role for ubiquitin in Tat-mediated transactivation of the HIV-1 promoter, Nat. Cell Biol. 5 (2003) 754–761.

[22] L. Naldini, U. Blömer, P. Gallay, et al., In vivo gene delivery and stable transduction of nondividing cells by a lentiviral vector, Science 272 (1996) 263–267.

[23] R. Zufferey, D. Nagy, R.J. Mandel, et al., Multiply attenuated lentiviral vector achieves efficient gene delivery in vivo, Nat. Biotechnol. 15 (1997) 871–875.

[24] J.W. Shih, W.T. Wang, T.Y. Tsai, et al., Critical role of RNA helicase DDX3 and its interactions with eIF4E/PABP1 in stress granule assembly and stress response, Biochem. J. 441 (2012) 119–129.

[25] A. Sharma, S. Awasthi, C.K. Harrod, et al., The Werner syndrome helicase is a cofactor for HIV-1 long terminal repeat transactivation and retroviral replication, J. Biol. Chem. 282 (2007) 12048–12057.

[26] R. Fujii, M. Okamoto, S. Aratani, et al., A role of RNA helicase A in *cis*-acting transactivation response element-mediated transcriptional regulation of human immunodeficiency virus type 1, J. Biol. Chem. 276 (2001) 5445–5451.

[27] C. Cocude, M.J. Truong, O. Billaut-Mulot, et al., A novel cellular RNA helicase, RH116, differentially regulates cell growth, programmed cell death and human immunodeficiency virus type 1 replication, J. Gen. Virol. 84 (2003) 3215–3225.

[28] R. Soto-Rifo, P.S. Rubilar, T. Limousin, et al., DEAD-box protein DDX3 associates with eIF4F to promote translation of selected mRNAs, EMBO J. 31 (2012) 3745–3756.

[29] C. Bolinger, A. Sharma, D. Singh, et al., RNA helicase A modulates translation of HIV-1 and infectivity of progeny virions, Nucleic Acids Res. 38 (2010) 1686–1696.

JVI
Journals.ASM.org

Distinct HIV-1 Escape Patterns Selected by Cytotoxic T Cells with Identical Epitope Specificity

Yuichi Yagita,[a] Nozomi Kuse,[a] Kimiko Kuroki,[b] Hiroyuki Gatanaga,[a,c] Jonathan M. Carlson,[d] Takayuki Chikata,[a] Zabrina L. Brumme,[e,f] Hayato Murakoshi,[a] Tomohiro Akahoshi,[a] Nico Pfeifer,[d] Simon Mallal,[g] Mina John,[g] Toyoyuki Ose,[b] Haruki Matsubara,[b] Ryo Kanda,[b] Yuko Fukunaga,[b] Kazutaka Honda,[a] Yuka Kawashima,[a] Yasuo Ariumi,[a] Shinichi Oka,[a,c] Katsumi Maenaka,[b] Masafumi Takiguchi[a]

Center for AIDS Research, Kumamoto University, Chuo-ku, Kumamoto, Japan[a]; Laboratory of Biomolecular Science, Faculty of Pharmaceutical Sciences, Hokkaido University, Kita-ku, Sapporo, Japan[b]; AIDS Clinical Center, National Center for Global Health and Medicine, Shinjuku-ku, Tokyo, Japan[c]; eScience Group, Microsoft Research, Los Angeles, California[d]; Faculty of Health Sciences, Simon Fraser University, Burnaby BC, Canada[e]; British Columbia Centre for Excellence in HIV/AIDS, Vancouver, BC, Canada[f]; Institute for Immunology & Infectious Diseases, Murdoch University, Murdoch, Western Australia, Australia[g]

Pol283-8-specific, HLA-B*51:01-restricted, cytotoxic T cells (CTLs) play a critical role in the long-term control of HIV-1 infection. However, these CTLs select for the reverse transcriptase (RT) I135X escape mutation, which may be accumulating in circulating HIV-1 sequences. We investigated the selection of the I135X mutation by CTLs specific for the same epitope but restricted by HLA-B*52:01. We found that Pol283-8-specific, HLA-B*52:01-restricted CTLs were elicited predominantly in chronically HIV-1-infected individuals. These CTLs had a strong ability to suppress the replication of wild-type HIV-1, though this ability was weaker than that of HLA-B*51:01-restricted CTLs. The crystal structure of the HLA-B*52:01-Pol283-8 peptide complex provided clear evidence that HLA-B*52:01 presents the peptide similarly to HLA-B*51:01, ensuring the cross-presentation of this epitope by both alleles. Population level analyses revealed a strong association of HLA-B*51:01 with the I135T mutant and a relatively weaker association of HLA-B*52:01 with several I135X mutants in both Japanese and predominantly Caucasian cohorts. An *in vitro* viral suppression assay revealed that the HLA-B*52:01-restricted CTLs failed to suppress the replication of the I135X mutant viruses, indicating the selection of these mutants by the CTLs. These results suggest that the different pattern of I135X mutant selection may have resulted from the difference between these two CTLs in the ability to suppress HIV-1 replication.

HIV-1-specific cytotoxic T cells (CTLs) play an important role in the control of HIV-1 replication (1–8); however, they also select immune escape mutations (9, 10). Population level adaptation of HIV to human leukocyte antigen (HLA) has been demonstrated (11–15), suggesting that HIV-1 can successfully adapt to immune responses previously effective against it.

It is well known that particular mutations can be selected by CTLs specific for a single HIV-1 epitope. On the other hand, studies on HLA-associated HIV-1 polymorphisms have revealed examples of particular mutations associated with multiple HLA class I alleles (16–21), suggesting that the same mutation can be selected by CTLs carrying different specificities in some cases. However, the selection of the same mutation by CTLs specific for different HIV-1 epitopes has rarely been reported. The change from Ala to Pro at residue 146 of Gag (A146P) is a well-analyzed case. A146P is an escape selected by not only HLA-B*57-restricted, ISW9-specific CTLs (22) but also by HLA-B*15:10-restricted and HLA-B*48:01-restricted CTLs (15, 23, 24), although the latter CTLs selected it by different mechanisms. The replacement of Thr with Asn at residue 242 (T242N) of Gag is another case. This mutant is selected by HLA-B*58:01-restricted and HLA-B*57-restricted CTLs specific for the TW10 epitope in HIV-1 clade B- and C-infected individuals (25–27).

The presence of Pol283-8(TAFTIPSI: TI8)-specific, HLA-B*51:01-restricted CTLs is associated with low viral loads in HIV-1-infected Japanese hemophiliacs, supporting an important role in the long-term control of HIV-1 infection (28). We previously showed that the frequency of a mutation at position 135 (I135X) of reverse transcriptase (RT) is strongly correlated with the prevalence of HLA-B*51 among nine cohorts worldwide and that this mutation is selected by Pol283-8(TAFTIPSI: TI8)-specific, HLA-B*51:01-restricted CTLs (15). Of these cohorts, a Japanese one showed the highest frequency of the I135X mutation in HLA-B*51:01 negatives (66% in a Japanese cohort and 11 to 29% in other cohorts). This finding may be explained by the fact that the Japanese cohort has the highest prevalence of HLA-B*51:01 among these cohorts. Another possibility is that this mutation is selected by HIV-1-specific CTLs restricted by other HLA alleles, which are highly frequent among Japanese individuals but infrequent in or absent from other populations. To clarify the latter possibility, we first analyzed the association of the I135X mutation with other HLA class I alleles in a Japanese cohort and found this mutation also to be associated with HLA-B*52:01. We next sought to identify an HLA-B*52:01-restricted CTL epitope including RT135 and found that both HLA-B*51:01 and -B*52:01 can present the same epitope, Pol283-8. Using population level analyses of Japanese and Caucasian cohorts, we identified HLA-B*51:01- and HLA-B*52:01-specific polymorphisms at RT codon 135 (position 8 of this epitope) and characterized differential pathways of escape between these two alleles. In addition, we assessed the *in vitro* ability of HLA-B*52:01- and HLA-B*51:01-restricted CTLs to se-

Received 20 September 2012 **Accepted** 26 November 2012
Published ahead of print 12 December 2012
Address correspondence to Masafumi Takiguchi, masafumi@kumamoto-u.ac.jp.
Y.Y., N.K., and K.K. contributed equally to this study.
Supplemental material for this article may be found at http://dx.doi.org/10.1128/JVI.02572-12.

doi:10.1128/JVI.02572-12

lect I135X mutants and elucidated the crystal structure of the HLA-B*52:01-Pol283-8 peptide complex.

MATERIALS AND METHODS

Patients. Two hundred fifty-seven chronically HIV-1-infected, antiretroviral-naïve Japanese individuals were recruited for the present study, which was approved by the ethics committees of Kumamoto University and the National Center for Global Health and Medicine, Japan. Written informed consent was obtained from all subjects according to the Declaration of Helsinki.

In addition, HLA-associated immune selection pressure at RT codon 135 was investigated in the International HIV Adaptation Collaborative (IHAC) cohort, comprising >1,200 chronically HIV-infected, antiretroviral-naïve individuals from Canada, the United States, and Western Australia (19). The majority of the IHAC participants were Caucasian, and the HIV subtype distribution was >95% subtype B.

HIV-1 clones. An infectious proviral clone of HIV-1, pNL-432, and its mutant form pNL-M20A (containing a substitution of Ala for Met at residue 20 of Nef) were previously reported (29). Pol283-8 mutant viruses (Pol283-8L, -8T, -8V, and 8R) were previously generated on the basis of pNL-432 (15, 28).

Generation of CTL clones. Pol283-8-specific, HLA-B*52:01-restricted CTL clones were generated from HIV-1-specific, bulk-cultured T cells by limiting dilution in U-bottom 96-well microtiter plates (Nunc, Roskilde, Denmark). Each well contained 200 μl of the cloning mixture (about 1×10^6 irradiated allogeneic peripheral blood mononuclear cells (PBMCs) from healthy donors and 1×10^5 irradiated C1R-B*52:01 cells prepulsed with the corresponding peptide at 1 μM in RPMI 1640 supplemented with 10% human plasma and 200 U/ml human recombinant interleukin-2).

Intracellular cytokine staining (ICS) assay. PBMCs from HIV-1-seropositive HLA-B*52:01$^+$ HLA-B*51:01$^-$ individuals were cultured with each peptide (1 μM). Two weeks later, the cultured cells were stimulated with C1R-B*52:01 cells or those prepulsed with Pol283-8 peptide (1 μM) for 60 min, and then they were washed twice with RPMI 1640 containing 10% fetal calf serum (RPMI 1640-10% FCS). Subsequently, brefeldin A (10 μg/ml) was added. After these cells had been incubated for 6 h, they were stained with an anti-CD8 monoclonal antibody (MAb; Dako Corporation, Flostrup, Denmark), fixed with 4% paraformaldehyde, and then permeabilized with permeabilization buffer. Thereafter, the cells were stained with an anti-gamma interferon (IFN-γ) MAb (BD Bioscience). The percentage of CD8$^+$ cells positive for intracellular IFN-γ was analyzed by using a FACS-Cant II (BD Biosciences, San Jose, CA). All flow cytometric data were analyzed with FlowJo software (Tree Star, Inc., Ashland, OR).

Identification of 11-mer peptide recognized by HLA-B*52:01-restricted CD8$^+$ T cells. We identified an 11-mer peptide recognized by HLA-B*52:01-restricted CD8$^+$ T cells as follows. We stimulated PBMCs from a chronically HIV-1-infected HLA-B*52:01$^+$ donor (KI-069) with a peptide cocktail including overlapping 17-mer peptides covering RT135 and cultured the cells for 14 days. The cells in bulk culture were assessed by performing an ICS assay for C1R-HLA-B*52:01 cells prepulsed with each of these 17-mer peptides. The bulk-cultured cells recognized the target cells prepulsed with two of the 17-mer peptides assessed, Pol17-47 (KDFRKYTAFTIPSINNE) and Pol17-48 (TAFTIPSI NNETPGIRT). Further analysis with 11-mer overlapping peptides covering the Pol17-48 sequence showed that these bulk-cultured cells recognized the target cells prepulsed with Pol11-142 (TAFTIPSINNE) but not those prepulsed with Pol11-143 (FTIPSINNETP).

Assay of cytotoxicity of CTL clones to target cells prepulsed with the epitope peptide or infected with a vaccinia virus–HIV-1 recombinant. The cytotoxicity of Pol283-8-specific, HLA-B*52:01-restricted CTL clones to C1R cells expressing HLA-B*52:01 (C1R-B*52:01), which were previously generated (30), and prepulsed with peptide or infected with a vaccinia virus-HIV-1Gag/Pol recombinant was determined by the standard ^{51}Cr release assay described previously (31). In brief, the infected cells were incubated with 150 μCi Na$_2{}^{51}$CrO$_4$ in saline for 60 min and then washed three times with RPMI 1640 medium containing 10% newborn calf serum. Labeled target cells (2×10^3/well) were added to each well of a U-bottom 96-well microtiter plate (Nunc, Roskilde, Denmark) with the effector cells at an effector-to-target (E/T) cell ratio of 2:1. The cells were then incubated for 6 h at 37°C. The supernatants were collected and analyzed with a gamma counter. Spontaneous ^{51}Cr release was determined by measuring the number of counts per minute (cpm) in supernatants from wells containing only target cells (cpm spn). Maximum ^{51}Cr release was determined by measuring the cpm in supernatants from wells containing target cells in the presence of 2.5% Triton X-100 (cpm max). Specific lysis was defined as (cpm exp − cpm spn)/(cpm max − cpm spn) × 100, where cpm exp is the number of cpm in the supernatant in the wells containing both target and effector cells.

Enzyme-linked immunospot (ELISPOT) assay. Cryopreserved PBMCs of chronically HIV-1-infected HLA-B*52:01$^+$ individuals were plated in 96-well polyvinylidene plates (Millipore, Bedford, MA) that had been precoated with 5 μg/ml anti-IFN-γ MAb 1-DIK (Mabtech, Stockholm, Sweden). The appropriate amount of each peptide (100 or 10 nM) was added in a volume of 50 μl, and then PBMCs were added at 1×10^5 cells/well in a volume of 100 μl. The plates were incubated for 40 h at 37°C in 5% CO$_2$ and then washed with phosphate-buffered saline (PBS) before the addition of biotinylated anti-IFN-γ MAb (Mabtech) at 1 μg/ml. After the plates had been incubated at room temperature for 100 min and then washed with PBS, they were incubated with streptavidin-conjugated alkaline phosphatase (Mabtech) for 40 min at room temperature. Individual cytokine-producing cells were detected as dark spots after a 20-min reaction with 5-bromo-4-chloro-3-indolylphosphate and nitroblue tetrazolium by using an alkaline phosphatase-conjugate substrate (Bio-Rad, Richmond, CA). The spots were counted by an Eliphoto-Counter (Minerva Teck, Tokyo, Japan). PBMCs without peptide stimulation were used as a negative control. Positive responses were defined as those greater than the mean of the negative-control wells plus 2 standard deviations (SD) (the number of spots in wells without peptides).

HIV-1 replication suppression assay. The ability of HIV-1-specific CTLs to suppress HIV-1 replication was examined as previously described (32). CD4$^+$ T cells isolated from PBMCs derived from an HIV-1-seronegative individual with HLA-B*52:01, HLA-B*51:01, or both were cultured. After the cells had been incubated with the desired HIV-1 clones for 4 h at 37°C, they were washed three times with RPMI 1640-10% FCS medium. The HIV-1-infected CD4$^+$ T cells were then cocultured with Pol283-8-specific CTL clones. From day 3 to day 7 postinfection, culture supernatants were collected and the concentration of p24 antigen (Ag) in them was measured by use of an enzyme-linked immunosorbent assay kit (HIV-1 p24 Ag ELISA kit; ZeptoMetrix).

HLA stabilization assay with RMA-S cells expressing HLA-B*52:01 or HLA-B*51:01. The peptide-binding activity of HLA-B*52:01 or HLA-B*51:01 was assessed by performing an HLA stabilization assay with RMA-S cells expressing HLA-B*52:01 (RMA-S-B*52:01) or HLA-B*51:01 (RMA-S-B*51:01) as described previously (33). Briefly, RMA-S-B*51:01 and RMA-S-B*52:01 cells were cultured at 26°C for 16 to 24 h. The cells (2×10^5) in 50 μl of RPMI 1640 supplemented with 5% FCS (RPMI–5% FCS) were incubated at 26°C for 3 h with 50 μl of a solution of peptides at 10^{-3} to 10^{-7} M and then at 37°C for 3 h. After having been washed with RPMI–5% FCS, the cells were incubated for 30 min on ice with an appropriate dilution of TP25.99 MAb. After two washings with RPMI–5% FCS, they were incubated for 30 min on ice with an appropriate dilution of fluorescein isothiocyanate (FITC)-conjugated anti-mouse Ig antibodies. Finally, the cells were washed three times with RPMI–5% FCS and the fluorescence intensity of the cells was measured by the FACS-Cant II. Relative mean fluorescence intensity (MFI) was calculated by subtracting the MFI of cells not peptide pulsed from that of the peptide-pulsed ones.

Sequencing of plasma RNA. Viral RNA was extracted from the plasma of chronically HIV-1-infected Japanese individuals by using a QIAamp

Mini Elute Virus spin kit (Qiagen). cDNA was synthesized from the RNA with Superscript II and random primer (Invitrogen). We amplified HIV RT and integrase sequences by nested PCR with RT-specific primers 5′-CCAAAAGTTAAGCAATGGCC-3′ and 5′-CCCATCCAAAGGAATGGAGG-3′ or 5′-CCTTGCCCCTGCTTCTGTAT-3′ for the first-round PCR and 5′-AGTTAGGAATACCACACCCC-3′ and 5′-GTAAATCCCCACCTCAACAG-3′ or 5′-AATCCCCACCTCAACAGAAG-3′ for the second-round PCR and integrase-specific primers 5′-ATCTAGCTTTGCAGGATTCGGG-3′ and 5′-CCTTAACCGTAGTACTGGTG-3′ or 5′-CCTGATCTCTTACCTGTCC-3′ for the first-round PCR and 5′-AAAGGTCTACCTGGCATGGG-3′ or 5′-TTGGAGAGCAATGGCTAGTG-3′ and 5′-AGTCTACTTGTCCATGCATGGC-3′ for the second-round PCR. PCR products were sequenced directly or cloned with a TOPO TA cloning kit (Invitrogen) and then sequenced. Sequencing was done with a BigDye Terminator v1.1. cycle sequencing kit (Applied Biosystems) and analyzed by an ABI PRISM 310 Genetic Analyzer.

Statistical analysis with phylogenetically corrected odds ratios. Strength of selection was measured by using a phylogenetically corrected odds ratio as previously described (19). Briefly, the odds of observing a given amino acid (e.g., 135V) was modeled as $P/(1 - P) = (a \times X) + (b \times T)$, where P is the probability of observing 135V in a randomly selected individual, X is a binary (0/1) variable representing whether or not an individual expresses the HLA allele in question (e.g., B*52:01), and T equals 1 if the transmitted/founder virus for that individual carried 135V and −1 otherwise. Because the transmitted/founder virus is unknown, we averaged over all possibilities by using weights informed by a phylogeny that was constructed from the RT sequences of all of the individuals in the study. The parameters a and b were determined by using iterative maximum-likelihood methods. The maximum-likelihood estimate of a is an estimate of the natural logarithm of the odds ratio of observing 135V in individuals expressing X versus individuals not expressing X, conditioned on the individuals' (unobserved) transmitted/founder virus. P values are estimated by using a likelihood ratio test that compares the above model to a null model in which a equals 0.

To compare the odds of selection between two cohorts, we modified the phylogenetically corrected logistic regression model to include a cohort term, $Z = X \times Y$, where X is the HLA allele, and Y is a 0/1 variable that indicates cohort membership, yielding $P/(1 - P) = (a \times X) + (b \times T) + (c \times Z)$, as previously described (19, 34). A P value testing if the odds of escape are different in the two cohorts was estimated by using a likelihood ratio test that compared this model to a null model where c equals 0.

Generation of HLA class I tetramers. HLA class I-peptide tetrameric complexes (tetramer) were synthesized as described previously (31, 35). The Pol283-8 peptide was used for the refolding of HLA-B*51:01 or HLA-B*52:01 molecules. Phycoerythrin (PE)-labeled streptavidin (Molecular Probes) was used for generation of the tetramers.

Tetramer binding assay. HLA-B*51:01-restricted and HLA-B*52:01-restricted CTL clones were stained at 37°C for 30 min with PE-conjugated HLA-B*51:01-tetramer and HLA-B*52:01-tetramer, respectively, at concentrations of 5 to 1,000 nM. After two washes with RPMI 1640 medium supplemented with 10% FCS (RPMI 1640–10% FCS), the cells were stained with FITC-conjugated anti-CD8 MAb at 4°C for 30 min, followed by 7-amino-actinomycin D at room temperature for 10 min. After two more washes with RPMI 1640–10% FCS, the cells were analyzed by the FACS-Cant II flow cytometer. The tetramer concentration that yielded the half-maximal MFI (the EC_{50}) was calculated by probit analysis.

Crystallization, data collection, and structure determination. Soluble HLA-B*52:01 (with beta-2 microglobulin and peptide TAFTIPSI) was prepared as described above. Prior to crystallization trials, HLA-B*52:01 was concentrated to a final concentration of 20 mg ml^{-1} in 20 mM Tris-HCl (pH 8.0) buffer containing 250 mM NaCl. This was done with a Millipore centrifugal filter device (Amicon Ultra-4, 10-kDa cutoff; Millipore). Screening for crystallization was performed with commercially available polyethylene glycol (PEG)-based screening kits, PEGs and PEGs II suites (Qiagen). Thin needle crystals were observed from PEGs II suite 23 (0.2 M sodium acetate, 0.1 M HEPES [pH 7.5], and 20% PEG 3000). Several conditions were further screened by the hanging-drop method with 24-well VDX plates (Hampton Research) by mixing 1.5 μl protein solution and 1.5 μl reservoir to be equilibrated against reservoir solution (0.5 ml) at 293 K. Best crystals were grown from macro seeding with the initial crystals obtained with 0.2 M sodium acetate, 0.1 M Bis Tris propane [pH 7.5], and 20% PEG 3350.

The data set was collected at beamline BL41XU of SPring-8 with Rayonix charge-coupled device detector MX225HE. Prior to diffraction data collection, crystals were cryoprotected by transfer to a solution containing 25% (vol/vol) glycerol and incubation in it for a few seconds, followed by flash cooling. The data sets were integrated with XDS (36) and then merged and scaled by using Scala (37). HLA-B*52:01 crystals belonged to space group $P2_12_12_1$, with unit cell parameters $a = 69.0$ Å, $b = 83.3$ Å, and $c = 170.3$ Å. Based on the values of the Matthews coefficient (V_M) (38), we estimated that there were two protomers in the asymmetric unit with a V_M value of 1.37 A^3/Da (Vsolv = 10.5%). For details of the data collection and processing statistics, see Table S1 in the supplemental material.

The structure was solved by the molecular replacement method with Molrep (39). The crystal structure of HLA-B*51:01 (PDB ID: 1E28) was used as a search model. Structure refinement was carried out by using Refmac5 (40) and phenix (41). The final model was refined to an Rfree factor of 34.7% and an R factor of 29.5% with a root mean square deviation of 0.014 Å in bond length and 1.48° in bond angle for all reflections between resolutions of 38.8 and 3.1 Å. Table S1 in the supplemental material also presents a summary of the statistics for structure refinement. The stereochemical properties of the structure were assessed by Procheck (42) and COOT (43) and showed no residues in the disallowed region of the Ramachandran plot.

Protein structure accession number. Atomic coordinates and structure factors for HLA-B*52:01 have been deposited in the Protein Data Bank under accession code 3W39.

RESULTS

Association of I135X variants with HLA-B*52:01. To clarify the possibility that CTLs restricted by other HLA alleles select the I135X mutation, we investigated the association between other HLA alleles and this mutation in 257 Japanese individuals chronically infected with HIV-1. We found an association of HLA-B*52:01 with the I135X variant, though this association was weaker than that with HLA-B*51:01 (phylogenetically corrected ln odds ratio [lnOR] of 11.76 [$P = 8.77 \times 10^{-4}$] for B*52:01 versus an lnOR of 40.0 [$P = 5.78 \times 10^{-12}$] for B*51:01; Table 1). We also analyzed the effects of HLA-B*52:01 and HLA-B*51:01 in chronically HIV-1-infected Japanese individuals, excluding HLA-B*51:01$^+$ and HLA-B*52:01$^+$ individuals, respectively, and found a significant association between HLA-B*52:01 and I135X variants among 200 HLA-B*51:01-negative individuals with chronic HIV-1 infection ($P = 4.7 \times 10^{-4}$; see Fig. S1A in the supplemental material) and that of HLA-B*51:01 with the variants in 202 HLA-B*52:01-negative ones ($P = 5.3 \times 10^{-8}$; see Fig. S1B in the supplemental material). These results together imply that HLA-B*52:01-restricted CTLs selected this mutation.

Identification of HLA-B*52:01-restricted, Pol283-specific CTLs. To identify the HLA-B*52:01-restricted HIV-1 epitope including RT135, we first investigated whether overlapping peptides covering RT135 could elicit CD8$^+$ T cells specific for these peptides in chronically HIV-1-infected individuals. We identified CTLs recognizing the Pol11-142 (TAFTIPSINNE) peptide in a chronically HIV-1-infected HLA-B*52:01$^+$ donor, KI-069 (see Materials and Methods). Since the C terminus of HLA-B*52:01-binding peptides is known to be a hydrophobic residue (30, 44), we speculated that TAFTIPSI (Pol283-8) was the epitope peptide.

TABLE 1 HLA-B*52:01 and HLA-B*51:01 association with variation at RT135 in Japanese and Caucasian cohorts

		PlyloLOR[a]		Within-cohort *P* value		
HLA class I allele	RT135 target variable	Japanese	IHAC	Japanese	IHAC	*P* value comparing cohorts
B*51:01	T	13.70	4.53	4.66×10^{-6}	1.70×10^{-35}	0.042
B*52:01	T	−9.77	1.25	0.464	2.04×10^{-3}	0.62
B*51:01	I	−40.00	−5.71	5.78×10^{-12}	1.58×10^{-51}	0.052
B*52:01	I	−11.76	−3.06	8.77×10^{-4}	2.95×10^{-5}	0.52
B*51:01	V	−9.76	8.52	0.884	0.41	0.85
B*52:01	V	12.21	10.15	0.076	1.82×10^{-3}	0.037
B*51:01	R	12.08	13.02	0.038	2.36×10^{-3}	0.42
B*52:01	R	0.26	8.37	0.423	0.469	0.89
B*51:01	L	−0.89	3.21	1	0.038	0.17
B*52:01	L	−0.56	3.61	1	0.231	0.29
B*51:01	K	−0.71	−40.00	1	0.53	0.99
B*52:01	K	−0.69	−40.00	1	0.779	0.99
B*51:01	M	7.76	12.00	0.894	2.10×10^{-4}	0.34
B*52:01	M	11.09	−40.00	0.034	0.517	0.12

[a] PlyloLOR, phylogenetically corrected lnOR.

Indeed, bulk-cultured T cells that had been cultured for 2 weeks after stimulation with Pol17-48 recognized C1R-B*52:01 cells prepulsed with Pol283-8 peptide at a much lower concentration than those incubated with the Pol11-142 peptide (Fig. 1A), strongly suggesting that Pol283-8 is an epitope recognized by HLA-B*52:01-restricted CTLs. These findings were confirmed by ELISPOT assay with PBMCs from two HLA-B*52:01$^+$ individuals chronically infected with HIV-1 (Fig. 1B). To clarify whether this peptide was processed and presented by HLA-B*52:01, we investigated the killing activity of bulk-cultured T cells against HLA-B*52:01$^+$ target cells infected with a vaccinia virus–HIV-1 Gag/Pol recombinant. They killed target cells infected with this recombinant but not those infected with wild-type vaccinia virus (Fig. 1C), indicating that the Pol283-8 peptide was presented by

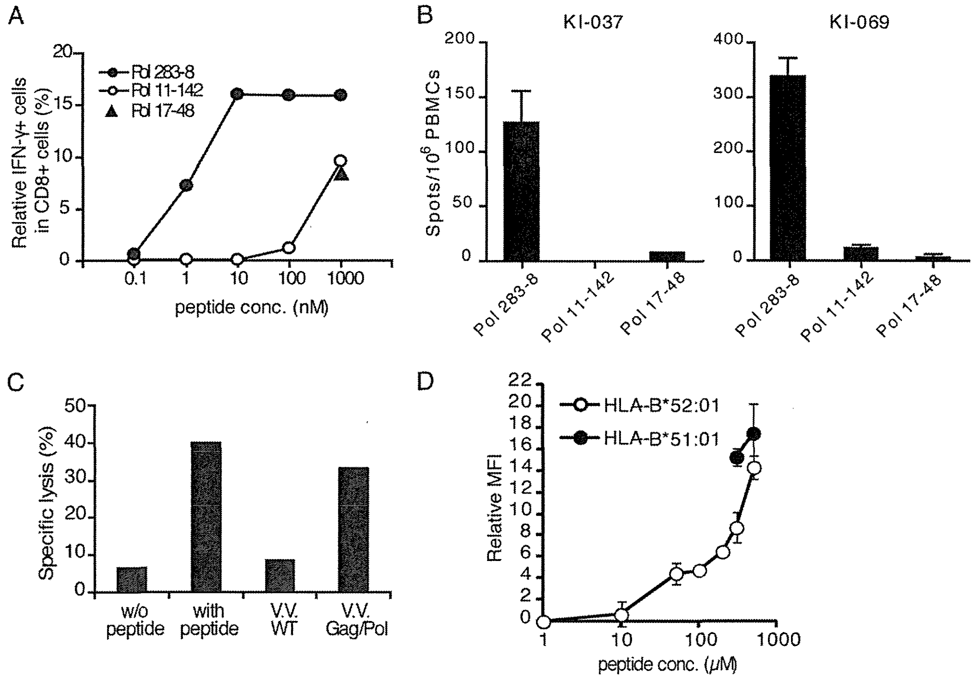

FIG 1 Identification of HLA-B*52:01-restricted Pol epitope. (A) Identification of the epitope peptide recognized by HLA-B*52:01-restricted CD8$^+$ T cells. Bulk T cells were cultured for 2 weeks after stimulation with the Pol17-48 peptide, and then the recognition of C1R-HLA-B*52:01 cells prepulsed with Pol17-48, Pol11-142, or Pol283-8 peptide was assessed by ICS assay. (B) Pol283-8 peptide recognition by T cells *ex vivo*. Recognition of the Pol17-48, Pol11-142, or Pol283-8 peptide by PBMCs from two HLA-B*52:01$^+$ individuals chronically infected with HIV-1 (KI-037 and KI-069) was analyzed by ELISPOT assay. A 100 nM concentration of each peptide was used. (C) Killing activity of Pol283-specific, HLA-B*52:01-restricted CD8$^+$ T cells against cells infected with a vaccinia virus–HIV-1 Gag/Pol recombinant. The killing activities of bulk-cultured T cells stimulated with Pol11-142 against target cells infected with a vaccinia virus–HIV-1 Gag/Pol recombinant (Gag/Pol) and against those infected with wild-type vaccinia virus (V.V. WT) are shown. (D) Binding of Pol283-8 peptide to HLA-B*52:01. Binding ability was measured by performing the HLA class I stabilization assay with RMA-S-B*52:01. RMA-S-B*51:01 cells were used as control cells for the Pol283-8 peptide.

TABLE 2 Pol283-8-specific CD8$^+$ T cells in chronically HIV-1-infected, HLA-B*52:01$^+$ individuals

Patient ID	HLA class I alleles		No. of CD4 cells/μl	No. of CD8 cells/μl	Viral load (no. of copies/ml)	Antiretroviral therapy	Relative IFN-γ$^+$/CD8$^+$ % in ICC assay	No. of spots/10^6 PBMCs in ELISPOT[a] assay
KI-037	A*24:02/–	B*52:01/40:02	465	973	76,000	–	64.1	150
KI-090	A*24:02/–	B*52:01/55:01	606	511	≤50	+	40.2	80
KI-106	A*24:02/33:03	B*52:01/07:01	433	890	≤50	+	1.4	<79
KI-126	A*24:02/31:01	B*52:01/40:01	465	NT[b]	36,000	–	60.4	<79
KI-130	A*24:02/–	B*52:01/07:02	351	1,275	14,000	–	0.0	<79
KI-167	A*24:02/–	B*52:01/54:01	455	909	26,000	–	0.0	<79
KI-067	A*24:02/–	B*52:01/48:01	234	1,198	89,000	–	10.9	<79
KI-071	A*24:02/31:01	B*52:01/40:06	292	1,134	48,000	–	0.7	<79
KI-076	A*02:01/24:01	B*52:01/40:01	136	252	14,000	–	61.0	80
KI-114	A*02:01/24:01	B*52:01/27:04	416	463	≤50	+	0.1	<79
KI-056	A*24:02/–	B*52:01/40:02	290	844	8,200	–	-0.1	<79
KI-108	A*24:02/–	B*52:01/–	373	481	NT	–	1.0	<79
KI-028	A*24:02/26:01	B*52:01/48:01	1,351	811	≤50	+	0.5	<79
KI-069	A*24:02/–	B*52:01/40:06	448	1,631	4,400	–	18.1	790

[a] More than the mean number of negative-control spots + 2 SD was defined as a positive response (positive response, >79 spots).

[b] NT, not tested.

HLA-B*52:01. We analyzed the binding of the Pol283-8 peptide to HLA-B*52:01 by using the HLA stabilization assay. The results demonstrated that this peptide bound to HLA-B*52:01 (Fig. 1D). These results together indicate that the Pol283-8 epitope can therefore be presented by both HLA-B*51:01 and HLA-B*52:01.

We investigated whether Pol283-8-specific CD8$^+$ T cells were elicited predominantly in chronically HIV-1-infected HLA-B*52:01$^+$ HLA-B*51:01$^-$ individuals. PBMCs from 14 of these individuals were analyzed by ICS assay with Pol283-8 peptide-stimulated culture cells, as well as by ELISPOT assay. The results of the ICS assay showed that 7 of these 14 HLA-B*52:01$^+$ HLA-B*51:01$^-$ patients had Pol283-specific CD8$^+$ T cells, whereas those of the ELISPOT assay with *ex vivo* PBMCs revealed that Pol283-specific CD8$^+$ T cells were detected in only four individuals (Table 2). These results suggest that the three individuals in whom the specific CTLs were detected by the ICS assay but not by the ELISPOT assay may have memory T cells. These results together indicate that Pol283-8 was recognized as an HLA-B*52:01-restricted immunodominant epitope in the HLA-B*52:01$^+$ individuals and support the idea that the I135X mutation was selected by HLA-B*52:01-restricted, Pol283-8-specific CD8$^+$ T cells.

Strong ability of HLA-B*52:01-restricted, Pol283-8-specific CD8$^+$ T cells to suppress HIV-1 replication. A previous study showed that HLA-B*51:01-restricted, Pol283-8-specific T cells have a strong ability to kill HIV-1-infected target cells and to suppress HIV-1 replication (31). Therefore, we expected that the HLA-B*52:01-restricted T cells also would have this strong ability. We generated HLA-B*52:01-restricted, Pol283-8-specific T cell clones and investigated their ability to kill peptide-pulsed or HIV-1-infected target cells. Clone 1E1 effectively killed C1R-B*52:01 cells prepulsed with the Pol283-8 peptide (Fig. 2A) and NL-432-infected CD4$^+$ T cells from an HLA-B*52:01$^+$ individual (Fig. 2B). Additional T cell clones also showed strong killing activity against NL-432-infected HLA-B*52:01$^+$ CD4$^+$ T cells (data not shown). In addition, we investigated the ability of these CTL clones to suppress HIV-1 replication. CD4$^+$ T cells derived from an HLA-B*52:01$^+$ individual were infected with NL-432 or M20A mutant virus, the latter of which has an amino acid substitution at position 20 of Nef and lacks the ability to downregulate the surface expression of HLA-A and -B molecules (Fig. 2C). Representative data on the 1E1 clone and summary data on four clones are shown in Fig. 2D and E, respectively. These CTL clones strongly suppressed the replication of both the NL432 and M20A mutant viruses, indicating that the HLA-B*52:01-restricted CTLs had a strong ability to suppress HIV-1 replication, as was the case with the HLA-B*51:01-restricted ones.

Recognition of I135X mutations by Pol283-8-specific, HLA-B*52:01-restricted CTLs. Four mutations (8T, 8L, 8R, and 8V) were observed predominantly at RT135 in chronically HIV-1-infected HLA-B*52:01$^+$ individuals (Fig. 3). These mutations may have been selected by Pol283-8-specific, HLA-B*52:01-restricted CTLs in these patients. We therefore investigated the ability of HLA-B*52:01-restricted CTLs to suppress the replication of these mutant viruses *in vitro*. The CTL clones failed to suppress the replication of the 8L, 8T, or 8R mutant, though they weakly suppressed that of the 8V virus at an E/T cell ratio of 1:1 (Fig. 4A). These results support the idea that these variants were escape mutations from the HLA-B*52:01-restricted CTLs. To clarify the mechanism by which the CTL clones failed to suppress the replication of these mutant viruses, we investigated the CTL clones for recognition of C1R-B*52:01 cells prepulsed with the mutant peptides. The CTL clones effectively recognized the 8V peptide at the same level as the wild-type peptide and the 8T and 8L peptides at less than that of the wild-type one, whereas they failed to recognize the 8R peptide (Fig. 4B). An ELISPOT assay with *ex vivo* PBMCs from KI-069 showed that Pol283-8-specific CTLs effectively recognized the 8I and 8V variants but not the other three mutant peptides (Fig. 4C), suggesting that Pol283-8-specific CTLs failed to recognize the 8T, 8L, and 8R peptides *in vivo*. The lack of recognition of these mutants by CTLs may be attributable to a failure of T cell receptor (TCR) recognition, the inability of the peptide to bind to HLA-B*52:01, and/or disruption of the processing of the epitope in HIV-1-infected cells.

Different pattern of RT135 mutation selection by two HLA alleles. As described above, HLA-B*51:01 and HLA-B*52:01 were associated with I135X in a Japanese population in which the prevalence of HLA-B*51:01 and B*52:01 alleles is relatively high (21.9 and 21.1%, respectively). In a Japanese cohort, out of the five

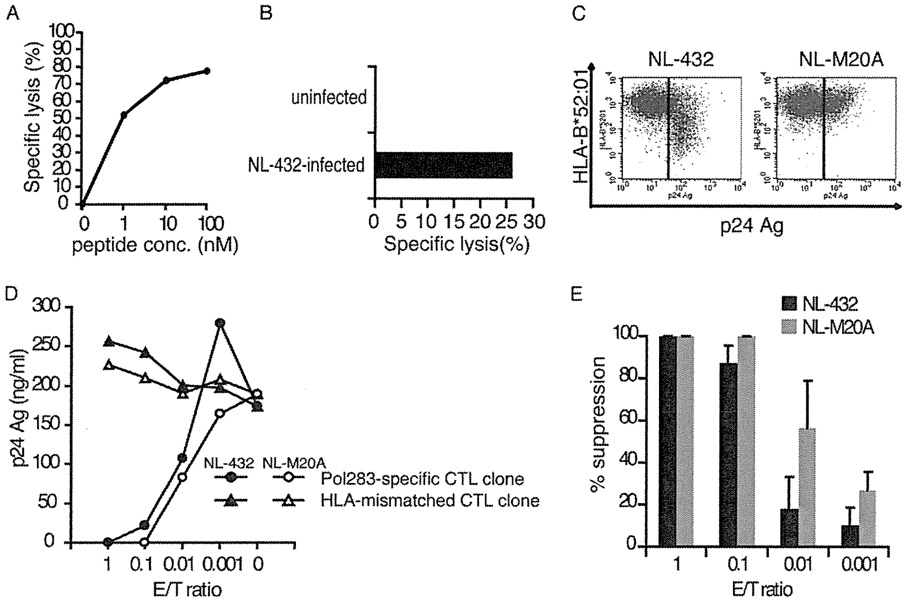

FIG 2 Abilities of HLA-B*52:01-restricted, Pol283-8-specific CD8$^+$ T cell clones to kill HIV-1-infected CD4$^+$ T cells and to suppress HIV-1 replication. (A) Killing activity of an HLA-B*52:01-restricted, Pol283-8-specific CD8$^+$ T cell clone against C1R-B*52:01 cells prepulsed with Pol283-8 peptides. The activity of an HLA-B*52:01-restricted, Pol283-8-specific CD8$^+$ T clone, 1E1, to kill C1R-B*52:01 cells was measured by performing a ^{51}Cr-release assay. (B) Killing activity of HLA-B*52:01-restricted, Pol283-8-specific CD8$^+$ T cell clone 1E1 against CD4$^+$ T cells infected with HIV-1. The ability of the clone to kill CD4$^+$ T cells infected with NL-432 was measured by performing a ^{51}Cr-release assay. (C) Downregulation of HLA-B*52:01 in HIV-1-infected CD4$^+$ T cells. CD4$^+$ T cells derived from an HLA-B*52:01$^+$ donor (HLA-A*11:01/A*24:02, HLA-B*52:01/B*52:01, and HLA-C*12:02/C*14:02) were infected with NL-432 and then cultured for 4 days. The cultured CD4$^+$ T cells were stained with anti-p24 Ag and TÜ109 anti-Bw4 MAbs. (D) Ability of an HLA-B*52:01-restricted, Pol283-8-specific CD8$^+$ T cell clone to suppress the replication of NL-432 and M20A mutant viruses. Suppressing ability was measured at four different E/T cell ratios (1:1, 0.1:1, 0.01:1, and 0.001:1). HIV-1-infected HLA-B*52:01$^+$ CD4$^+$ T cells were cocultured with an HLA-B*52:01-restricted, Pol283-8-specific CTL clone or an HLA-mismatched CTL clone at various E/T cell ratios. HIV-1 p24 Ag levels in the supernatant were measured on day 6 postinfection. (E) Summary of the ability of HLA-B*52:01-restricted, Pol283-8-specific CD8$^+$ T cell clones ($n = 4$) to suppress the replication of Nl-432 and M20A mutant viruses at four different E/T cell ratios.

amino acid mutations that can be generated by a one-nucleotide mutation from Ile, the T mutation was strongly associated with the presence of HLA-B*51:01 ($P = 4.66 \times 10^{-6}$), whereas HLA-B*52:01 was associated not with any single amino acid substitu-

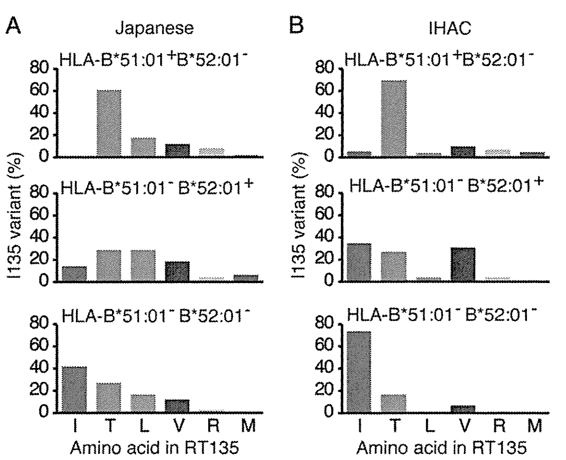

FIG 3 Amino acid variation at RT135 in Japanese individuals. (A) Frequency of the amino acid at RT135 in 51 HLA-B*51:01$^+$ HLA-B*52:01$^-$, 49 HLA-B*51:01$^-$ HLA-B*52:01$^+$, and 151 HLA-B*51:01$^-$ HLA-B*52:01$^-$ Japanese subjects. (B) Frequency of the amino acid at RT135 in 131 HLA-B*51:01$^+$ HLA-B*52:01$^-$, 26 HLA-B*51:01$^-$ HLA-B*52:01$^+$, and 1195 HLA-B*51:01$^-$ HLA-B*52:01$^-$ subjects in three predominantly Caucasian cohorts from Canada, the United States, and Western Australia (IHAC).

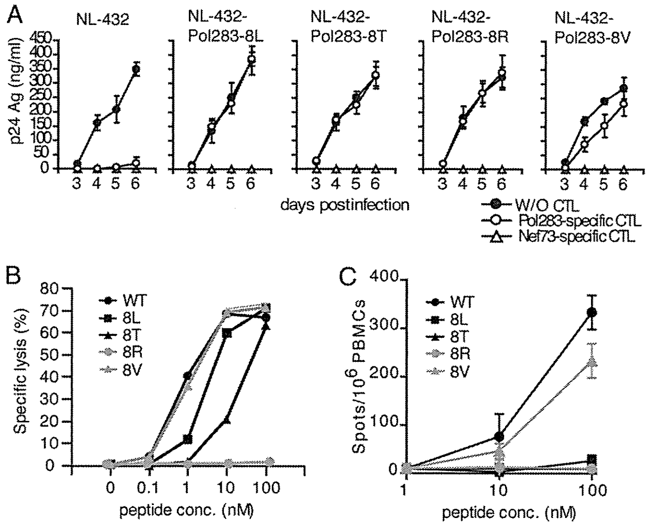

FIG 4 Ability of HLA-B*52:01-restricted, Pol283-8-specific CD8$^+$ T cell clones to suppress the replication of four mutant viruses. (A) Ability of an HLA-B*52:01-restricted, Pol283-8-specific CD8$^+$ T cell clone to suppress the replication of four (8L, 8T, 8R, and 8V) mutant viruses and NL-432. The abilities of an HLA-B*52:01-restricted, Pol283-8-specific CD8$^+$ T cell clone and an HLA-A*1101-restricted Nef73-specific T cell clone to suppress the replication of these viruses were measured at an E/T cell ratio of 1:1 on days 3 to 6. W/O, without. (B) Recognition by an HLA-B*52:01-restricted, Pol283-8-specific CD8$^+$ T cell clone of C1R-B*52:01 cells prepulsed with any one of the four mutant epitope peptides or the wild-type (WT) peptide (8I). (C) Recognition of mutant epitope peptides by *ex vivo* Pol283-8-specific CTLs. The recognition of the Pol283-8 peptide (WT) or the mutant epitope peptide by PBMCs from KI-069 was analyzed by ELISPOT assay.

tion but only with the non-I mutation ($P = 8.77 \times 10^{-4}$, Table 1). The distribution of amino acid variations at RT135 in the HLA-B*51:01^{+} HLA-B*52:01^{-} Japanese subjects was different from that in the HLA-B*51:01^{-} HLA-B*52:01^{+} ones (Fig. 3). These results suggest that the HLA-B*51:01-restricted CTLs strongly selected the 135T mutation but that the HLA-B*52:01-restricted ones selected a variety of different amino acids at this position in Japanese individuals.

We also analyzed the association of I135X mutations with HLA-B*52:01 and HLA-B*51:01 in three predominantly Caucasian cohorts from Canada, the United States, and Western Australia (International HIV Adaptation Collaborative [IHAC]) (19) comprising >1,200 subjects (Table 1). HLA-B*51:01 was very strongly associated with the I135X mutation (lnOR of 5.71; $P = 1.58 \times 10^{-51}$). Although only 2.1% of the IHAC cohort subjects expressed HLA-B*52:01, this allele was also associated with I135X (lnOR of 3.06; $P = 2.95 \times 10^{-5}$). The T mutation was strongly associated with HLA-B*51:01 ($P = 1.70 \times 10^{-35}$), whereas the T and V mutations were weakly associated with HLA-B*52:01 ($0.0005 < P < 0.005$). Thus, these results showed a similar selection of RT135 mutations by HLA-B*52:01 in the predominantly Caucasian cohort, despite a substantially lower frequency of HLA-B*52:01. The magnitude of the strength of selection by HLA-B*52:01 and HLA-B*51:01 on RT135 did not differ significantly between the two cohorts (Table 1). These results indicate that HLA-B*51:01 strongly selected 135T but that HLA-B*52:01 selected a variety of substitutions at this site (designated I135X) in both the Japanese and non-Japanese cohorts.

Comparison of TCR affinity and abilities of HLA-B*51:01-restricted and HLA-B*52:01-restricted CTLs to suppress HIV-1 replication. We investigated the TCR affinity of HLA-B*51:01-restricted and HLA-B*52:01-restricted CTL clones by using tetramers of the HLA-B*51:01-Pol283 peptide and the HLA-B*52:01-Pol283 peptide complex (HLA-B*51:01 and HLA-B*52:01 tetramers, respectively). The TCR affinity of these CTL clones was compared in terms of EC_{50}. The EC_{50} of the HLA-B*51:01-restricted CTL clones was significantly lower than that of the HLA-B*52:01-restricted CTL clones (Fig. 5A), suggesting that the former CTL clones had TCRs with a higher affinity for the ligand than those of the latter clones. These results imply that the HLA-B*51:01-restricted CTL clones could recognize the HIV-1-infected targets more effectively than HLA-B*52:01-restricted ones.

Since CD4^{+} T cells derived from an HLA-B*52:01 homozygous individual were used in the experiment shown in Fig. 2D and E, the ability of the HLA-B*52:01-restricted CTL clones to suppress the replication of NL-432 may have been overestimated. To evaluate and compare the abilities of HLA-B*51:01-restricted and HLA-B*52:01-restricted CTL clones to suppress the replication of NL-432, we used CD4^{+} T cells from individuals expressing HLA-B*51:01^{+}/B*52:01^{-}, HLA-B*51:01^{-}/B*52:01^{+}, or HLA-B*51:01^{+}/B*52:01^{+} (Fig. 5B). Two HLA-B*51:01-restricted CTL clones strongly inhibited the replication of HIV-1 in cultures of NL-432-infected HLA-B*51:01^{+}/B*52:01^{-} CD4^{+} T cells but not in those of HLA-B*51:01^{-}/B*52:01^{+} cells, whereas two HLA-B*52:01-restricted CTL clones strongly inhibited the replication of HIV-1 in cultures of NL-432-infected HLA-B*51:01^{-}/B*52:01^{+} CD4^{+} T cells but not in those of HLA-B*51:01^{+}/B*52:01^{-} cells (Fig. 5B, left and middle). The ability of the HLA-B*51:01-restricted CTL clones to suppress the replication of HIV-1 was greater than that of the HLA-B*52:01-restricted CTL clones. This was confirmed by the experiment with HLA-B*51:01^{+}/B*52:01^{+} CD4^{+} T cells (Fig. 5B, right). Although both HLA-B*51:01-restricted and HLA-B*52:01-restricted CTL clones strongly inhibited the replication of HIV-1 in the cultures of NL-432-infected HLA-B*51:01^{+}/B*52:01^{+} CD4^{+} T cells, the former clones exhibited a greater ability to suppress the replication of HIV-1 than did the latter cells. These results indicate that the HLA-B*51:01-restricted CTL clones had a stronger ability to suppress HIV-1 replication than the HLA-B*52:01-restricted clones. Taken together, both our *in vitro* and our *in vivo* (population level HLA-association) data suggest that immune pressure on RT135 by HLA-B*51:01-restricted T cells was stronger than that imposed by HLA-B*52:01-restricted cells.

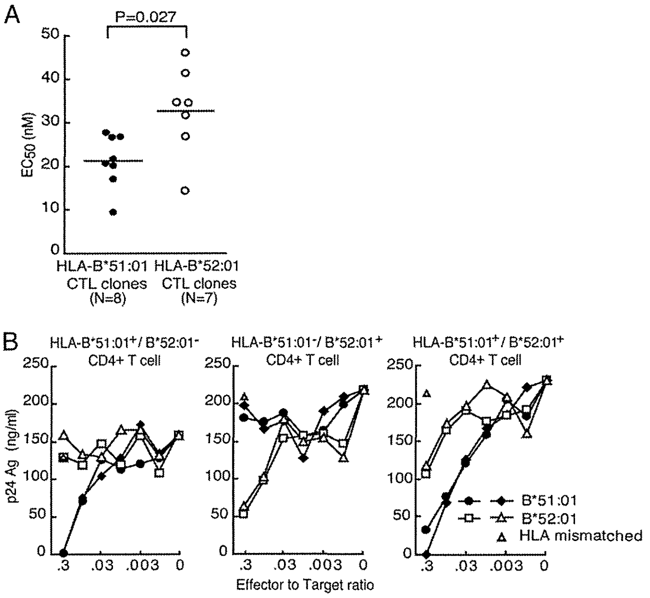

FIG 5 Differences between HLA-B*51:01-restricted and HLA-B*52:01-restricted CD8^{+} T cell clones in TCR avidity and the ability to suppress HIV-1 replication. (A) TCR avidity of the HLA-B*51:01-restricted and HLA-B*52:01-restricted CTL clones expressed as EC_{50}. The ability of the TCRs of HLA-B*51:01-restricted and HLA-B*52:01-restricted CTL clones to bind HLA-B*51:01 tetramers and HLA-B*52:01 tetramers, respectively, was measured in terms of the MFI of each CTL clone stained with the tetramers at concentrations of 5 to 1,000 nM. (B) The ability of two HLA-B*51:01-restricted and two HLA-B*52:01-restricted CD8^{+} T cell clones to suppress HIV-1 was measured at six different E/T cell ratios (0.3:1, 0.1:1, 0.03:1, 0.01:1, 0.003:1, and 0.001:1). CD4^{+} T cells from individuals expressing HLA-B*51:01^{+}/B*52:01^{-}, HLA-B*51:01^{-}/B*52:01^{+}, or HLA-B*51:01^{+}/B*52:01^{+} were infected with NL-432 and then cocultured with a given Pol283-8-specific CTL clone or an HLA-mismatched CTL clone. HIV-1 p24 Ag levels in the supernatant were measured on day 5 postinfection.

Structural basis of the difference in recognition between HLA-B*52:01- and HLA-B*51:01-restricted CTLs. In order to investigate the structural basis of the difference in recognition between HLA-B*52:01- and HLA-B*51:01-restricted CTLs, we performed a crystallographic study of the HLA-B*52:01 molecule complexed with the Pol283-8 peptide. The recombinant HLA-B*52:01 protein was crystallized, and by using the molecular replacement method, the three-dimensional structure of HLA-B*52:01 complexed with the Pol283-8 peptide was successfully determined. The crystal and statistical data are summarized in Table S1 in the supplemental material. The overall structure and peptide-binding mode were similar to those of HLA-B*51:01 complexed with the same Pol283-8 peptide (Fig. 6A and B), which

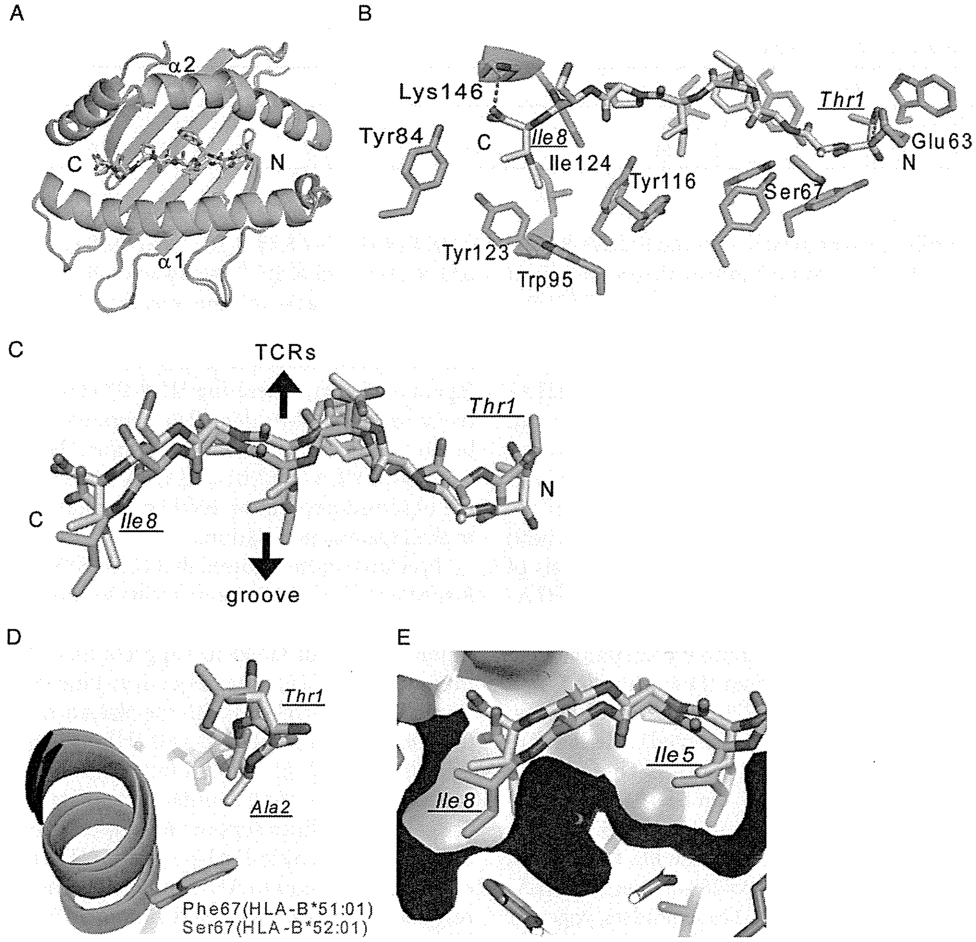

FIG 6 Structural comparison of HLA-B*52:01 and HLA-B*51:01 molecules complexed with the Pol283-8 peptide. (A) Crystal structures of HLA α1-α2 domains complexed with the Pol283-8 peptide (stick model) on the HLA-B*52:01 (green, yellow) and HLA-B*51:01 (cyan, cyan) complexes. This same coloring also applies to panels B to E. (B) Pol283-8 peptide and interacting side chains on the HLA-B*52:01 complex. Hydrogen bonds are shown as blue dotted lines. (C) Comparison of the Pol283-8 peptide conformations of HLA-B*52:01 and HLA-B*51:01 complexes. (D) N-terminal side of HLA-B*52:01 and HLA-B*51:01 complexes. (E) C-terminal side of HLA-B*52:01 and HLA-B*51:01 complexes. Surface presentation for the α1-α2 domains is shown in gray.

we had previously reported (45). This finding explains the cross presentation of this peptide by both HLA alleles. On the other hand, there was a notable conformational difference in the N-terminal region of the peptide between the two alleles (Fig. 6C and D). The replacement of Phe67 of HLA-B*51:01 with Ser in HLA-B*52:01 makes a local space, causing the N-terminal region of the peptide (T1 and A2) to reside deeper in the peptide-binding groove. Furthermore, the Gln63Glu mutation in HLA-B*52:01 affords a new interaction with the T1 residue of the peptide. These changes would, to some extent, have hidden the side chains of T1 and A2 (flat surface) from the TCRs, which may have reduced their interactions with TCRs on the HLA-B*52:01-restricted CTLs. On the other hand, the conformation of the C-terminal region of the peptide complexed with HLA-B*51:01 or HLA-B*52:01 was similar, even though C-terminal Ile8 of the peptide exhibited shallower penetration of the hydrophobic groove in the case of HLA-B*52:01 than in that of HLA-B*51:01 (Fig. 6C and E). These results may indicate that the relatively flat surface of the N-terminal side of the peptide contributed to the lower affinity for TCRs in the case of HLA-B*52:01.

DISCUSSION

HLA-B*52:01 and HLA-B*51:01 differ by only two residues, at positions 63 and 67 (44). Substitutions at these residues affect the formation of the B pocket in the peptide-binding pocket (45), suggesting the possibility that HLA-B*52:01 has a peptide motif different from that of HLA-B*51:01. Indeed, HLA-B*52:01-binding peptides have P2 primary anchors that are different from HLA-B*51:01-binding ones (30, 46). Since the Pol283-8 epitope carries Ala at its second position and Ile at the C terminus of the peptide, it is likely that this peptide would effectively bind to HLA-B*51:01 but not to HLA-B*52:01. However, the results of the HLA stabilization assay demonstrated that the Pol283-8 peptide did effectively bind to HLA-B*52:01. Since the HLA-B*52:01-binding peptide is known to have Pro as its preferred P2 anchor residue, this peptide carrying Ala at position 2 may be capable of binding to HLA-B*52:01. A previous study showed cross-recognition of alloreactive T cells between HLA-B*51:01 and HLA-B*52:01 (47, 48), indicating that some self-peptides can be presented by both of these HLA class I molecules. The findings on the crystal structure

TABLE 3 Numbers and frequencies of individuals having I135X mutations in a Japanese cohort and a predominantly Caucasian cohort

Cohort	No./total no. (%) of individuals				
	B*51:01$^+$ B*52:01$^-$	B*51:01$^-$ B*52:01$^+$	B*51:01$^+$ B*52:01$^+$	B*51:01$^-$ B*52:01$^-$	Total
Japanese	51/51 (100)	42/49 (85.7)	5/5 (100)	88/151 (58.3)	186/256 (72.6)
Caucasian	125/131 (95.4)	17/26 (65.4)	0/0	331/1,198 (27.6)	473/1,355 (34.9)

of the HLA-B*52:01 molecule complexed with the Pol283-8 peptide clarified that HLA-B*52:01 could bind to the peptide in a fashion similar to but slightly different from that of HLA-B*51:01. These findings support the presentation of the Pol283-8 peptide by both HLA-B*52:01 and HLA-B*51:01.

Pol283-8-specific CD8$^+$ T cells were detected in 7 of 14 HLA-B*52:01$^+$ HLA-B*51:01$^-$ individuals chronically infected with HIV-1. A previous analysis showed that CD8$^+$ T cells specific for this epitope are frequently detected in HLA-B*51:01$^+$ individuals chronically infected with HIV-1 (49). These results, taken together, indicate that this epitope is immunodominant in both HLA-B*51:01$^+$ and HLA-B*52:01$^+$ individuals. The analysis of 257 Japanese individuals revealed an association between HLA-B*52:01 and a variety of nonconsensus residues at RT codon 135 (I135X). Specifically, variants 8T, 8L, 8R, and 8V predominated in HLA-B*52:01$^+$ individuals, suggesting that these mutations had been selected by HLA-B*52:01-restricted CTLs. The viral suppression assay revealed that the HLA-B*52:01-restricted CTLs failed to suppress the replication of these mutant viruses. These results support the idea that the I135X mutation can be selected by immune pressure via Pol283-8-specific CTLs in HLA-B*52:01$^+$ individuals. Our previous studies showed that the 8L, 8T, and 8R mutations affected the recognition by Pol283-8-specific, HLA-B*51:01-restricted CTL clones (15, 28). These studies, together with the present study, indicate that accumulation of 8L, 8T, and 8R mutations in the HIV-infected Japanese population may be due to immune pressure by both HLA-B*52:01-restricted and HLA-B*51:01-restricted CTLs. Our analysis of the crystal structure of the HLA-B*52:01-peptide complex demonstrated that position 8 of the Pol283-8 peptide was deeply packed into the hydrophobic groove. Whereas the 8L, 8T, and 8R substitutions likely had a relatively large effect on the structure of the complex, the 8V mutation, resulting in only the deletion of the small methyl group, caused only very limited changes. Thus, the structural analysis supports the idea that the 8L, 8T, and 8R mutations affected the TCR recognition of the peptide and/or its binding to HLA-B*52:01.

The present study confirmed previous studies of nine worldwide cohorts (15) and a Chinese cohort (50) that showed a strong association of I135X with HLA-B*51:01. The I135X mutation was found in 58.3 and 27.6% of HLA-B*51:01$^-$ HLA-B*52:01$^-$ Japanese and predominantly Caucasian individuals, respectively (Table 3), supporting greater population level accumulation of this mutation in Japanese than in other cohorts. Since the Japanese cohort included twice as many HLA-B*51:01$^+$ individuals as the IHAC cohort (21.9% of Japanese and 9.4% of Caucasians in IHAC), the difference in the I135X variant frequency between these two cohorts would be driven, to a large extent, by the higher HLA-B*51:01 prevalence in the former than in the latter. The association of HLA-B*52:01 with this mutation was much weaker than that of HLA-B*51:01 in both cohorts but still highly statistically significant (an lnOR of 11.7 [$P = 8.77 \times 10^{-4}$] versus an lnOR of 40.0 [$P = 5.78 \times 10^{-12}$] in the Japanese cohort and an lnOR of 3.06 [$P = 2.95 \times 10^{-5}$] versus an lnOR of 5.71 [$P = 1.58 \times 10^{-51}$] in IHAC). Because of the relatively low B*52:01$^+$ frequency (~2%) in IHAC, the effect of HLA-B*52:01 on the overall prevalence of I135X was relatively low in this cohort. In contrast, in the Japanese cohort, where the HLA-B*52:01$^+$ prevalence was relatively high (>20%), this allele represents a major driving force behind 135X selection in this cohort. Thus, selection pressure from both HLA-B*51:01 and HLA-B*52:01 likely contributed to the observed population level accumulation of I135X mutations in the Japanese population.

Previous studies showed that HLA-B*51:01-restricted, Pol283-8-specific CTLs have a strong ability to suppress HIV-1 replication *in vitro* (28) and that they suppressed the replication of the 8V mutant virus but failed to suppress that of the 8T, 8L, and 8R mutant viruses (15). The frequency of the Pol283-8-specific CTLs was inversely correlated with the plasma viral load in HLA-B*51:01$^+$ hemophiliacs infected with HIV-1 approximately 30 years ago (28). The 8T, 8L, and 8R mutations did not affect replication capacity, whereas the 8V mutation conferred a modest fitness cost (15). These findings support the suppression of the wild-type or 8V mutant virus by Pol283-8-specific CTLs as a major mechanism of slow progression to AIDS in Japanese hemophiliacs. This CTL response was also elicited in Chinese HLA-B*51:01$^+$ individuals infected with the 8V mutant virus; furthermore, a low viral load and a high CD4 count were significantly associated with the presence of at least one of three HLA-B*51:01-restricted CTL responses, including a Pol283-8-specific one (50). Thus, these findings support the idea that Pol283-8-specific CTLs play an important role in the control of HIV-1 infection.

The present study demonstrated that HLA-B*52:01-restricted, Pol283-8-specific CTLs also had a strong ability to suppress HIV-1 replication *in vitro* (80% suppression at an E/T cell ratio of 0.3:1). However, the ability of HLA-B*52:01-restricted CTLs to suppress the replication of HIV-1 was weaker than that of HLA-B*51:01-restricted CTLs (Fig. 5B). Inspection of the crystal structures of both HLA molecules complexed with the Pol283-8 peptide suggests that the relatively shallow penetration of the hydrophobic groove of HLA-B*52:01 by the C-terminal side of the peptide, in contrast to the tightly packed binding with HLA-B*51:01, may have resulted in an unstable conformation of the complex. Furthermore, Ser67 of HLA-B*52:01 would have provided more space and loose interactions with the peptide than in the case of the Phe of HLA-B*51:01. Interestingly, the Pol283-8 peptide would have displayed only side chains of Thr1 and Ser7, and some part of the main chains, to CTLs. Therefore, these results suggest that the unstable backbone conformation and side chain positions in the case of HLA-B*52:01 largely contributed to the lower TCR affinity than that afforded by HLA-B*51:01. These results support that selection pressure *in vivo* via the HLA-B*52:01-restricted CTLs would be weaker than that via the HLA-B*51:01-restricted CTLs. Indeed, the prevalence of I135X mutations in HLA-B*51:

01$^+$ individuals was higher than that in HLA-B*52:01$^+$ individuals. The difference in the pattern of escape mutant selection by these CTLs between the HLA-B*51:01$^+$ and HLA-B*52:01$^+$ individuals might also have been due to the difference in their abilities to suppress HIV-1 replication. However, it still remains unclear why the 8T mutant was predominantly selected in the HLA-B*51:01$^+$ but not in the HLA-B*52:01$^+$ individuals. Further studies are expected to clarify the mechanism to explain how these CTLs selected different patterns of mutations at RT135.

Previous studies showed that the T242N mutant was selected by HLA-B*58:01-restricted and HLA-B*57-restricted CTLs specific for TW10 epitope in HIV-1 clade B-infected and clade C-infected individuals (25–27). Herein we also showed that I135X was selected by Pol283-8-specific CTLs restricted by two different HLA class I molecules. However, the strength and the pattern of the selection of I135X was different between HLA-B*51:01 and HLA-B*52:01. The present study suggests that this difference in the selection pattern was associated with that between the HLA-B*51:01$^+$ and HLA-B*52:01$^+$ individuals in terms of the ability of Pol283-specific CTLs to suppress HIV-1 replication. Thus, we characterized and experimentally validated distinct HIV-1 escape patterns of CTLs with the same epitope specificity and provided evidence that the extremely high prevalence of 135X in circulating Japanese sequences is likely driven not by one but by two HLA-B alleles.

ACKNOWLEDGMENTS

We thank Sachiko Sakai for her secretarial assistance, as well as Richard Harrigan and the BC Centre for Excellence in HIV/AIDS for data access. The assistance of Jennifer Listgarten and Carl Kadie (Microsoft Research) with HLA allele interpretation is also gratefully acknowledged.

N.K. is a JSPS Research Fellow. Z.L.B. is a recipient of a Canadian Institutes of Health Research (CIHR) New Investigator Award and a Michael Smith Foundation for Health Research (MSFHR) Scholar award. This research was supported by the Global COE program Global Education and Research Center Aiming at the Control of AIDS, launched as a project commissioned by the Ministry of Education, Science, Sports, and Culture, Japan, and by grants-in-aid for scientific research from the Ministry of Education, Science, Sports and Culture, Japan (18390141 and 20390134).

We have no financial conflicts of interest.

REFERENCES

1. **Borrow P, Lewicki H, Hahn BH, Shaw GM, Oldstone MB.** 1994. Virus-specific CD8$^+$ cytotoxic T-lymphocyte activity associated with control of viremia in primary human immunodeficiency virus type 1 infection. J. Virol. 68:6103–6110.
2. **Koup RA, Safrit JT, Cao Y, Andrews CA, McLeod G, Borkowsky W, Farthing C, Ho DD.** 1994. Temporal association of cellular immune responses with the initial control of viremia in primary human immunodeficiency virus type 1 syndrome. J. Virol. 68:4650–4655.
3. **Rinaldo C, Huang XL, Fan ZF, Ding M, Beltz L, Logar A, Panicali D, Mazzara G, Liebmann J, Cottrill M.** 1995. High levels of anti-human immunodeficiency virus type 1 (HIV-1) memory cytotoxic T-lymphocyte activity and low viral load are associated with lack of disease in HIV-1-infected long-term nonprogressors. J. Virol. 69:5838–5842.
4. **Matano T, Shibata R, Siemon C, Connors M, Lane HC, Martin MA.** 1998. Administration of an anti-CD8 monoclonal antibody interferes with the clearance of chimeric simian/human immunodeficiency virus during primary infections of rhesus macaques. J. Virol. 72:164–169.
5. **Ogg GS, Jin X, Bonhoeffer S, Dunbar PR, Nowak MA, Monard S, Segal JP, Cao Y, Rowland-Jones SL, Cerundolo V, Hurley A, Markowitz M, Ho DD, Nixon DF, McMichael AJ.** 1998. Quantitation of HIV-1-specific cytotoxic T lymphocytes and plasma load of viral RNA. Science 279:2103–2106.
6. **Schmitz JE, Kuroda MJ, Santra S, Sasseville VG, Simon MA, Lifton MA, Racz P, Tenner-Racz K, Dalesandro M, Scallon BJ, Ghrayeb J, Forman MA, Montefiori DC, Rieber EP, Letvin NL, Reimann KA.** 1999. Control of viremia in simian immunodeficiency virus infection by CD8$^+$ lymphocytes. Science 283:857–860.
7. **Gandhi RT, Walker BD.** 2002. Immunologic control of HIV-1. Annu. Rev. Med. 53:149–172.
8. **Goulder PJ, Watkins DI.** 2008. Impact of MHC class I diversity on immune control of immunodeficiency virus replication. Nat. Rev. Immunol. 8:619–630.
9. **Borrow P, Lewicki H, Wei X, Horwitz MS, Peffer N, Meyers H, Nelson JA, Gairin JE, Hahn BH, Oldstone MB, Shaw GM.** 1997. Antiviral pressure exerted by HIV-1-specific cytotoxic T lymphocytes (CTLs) during primary infection demonstrated by rapid selection of CTL escape virus. Nat. Med. 3:205–211.
10. **Goulder PJ, Phillips RE, Colbert RA, McAdam S, Ogg G, Nowak MA, Giangrande P, Luzzi G, Morgan B, Edwards A, McMichael AJ, Rowland-Jones S.** 1997. Late escape from an immunodominant cytotoxic T-lymphocyte response associated with progression to AIDS. Nat. Med. 3:212–217.
11. **Goulder PJ, Brander C, Tang Y, Tremblay C, Colbert RA, Addo MM, Rosenberg ES, Nguyen T, Allen R, Trocha A, Altfeld M, He S, Bunce M, Funkhouser R, Pelton SI, Burchett SK, McIntosh K, Korber BT, Walker BD.** 2001. Evolution and transmission of stable CTL escape mutations in HIV infection. Nature 412:334–338.
12. **Moore CB, John M, James IR, Christiansen FT, Witt CS, Mallal SA.** 2002. Evidence of HIV-1 adaptation to HLA-restricted immune responses at a population level. Science 296:1439–1443.
13. **Draenert R, Le Gall S, Pfafferott KJ, Leslie AJ, Chetty P, Brander C, Holmes EC, Chang SC, Feeney ME, Addo MM, Ruiz L, Ramduth D, Jeena P, Altfeld M, Thomas S, Tang Y, Verrill CL, Dixon C, Prado JG, Kiepiela P, Martinez-Picado J, Walker BD, Goulder PJ.** 2004. Immune selection for altered antigen processing leads to cytotoxic T lymphocyte escape in chronic HIV-1 infection. J. Exp. Med. 199:905–915.
14. **Leslie A, Kavanagh D, Honeyborne I, Pfafferott K, Edwards C, Pillay T, Hilton L, Thobakgale C, Ramduth D, Draenert R, Le Gall S, Luzzi G, Edwards A, Brander C, Sewell AK, Moore S, Mullins J, Moore C, Mallal S, Bhardwaj N, Yusim K, Phillips R, Klenerman P, Korber B, Kiepiela P, Walker B, Goulder P.** 2005. Transmission and accumulation of CTL escape variants drive negative associations between HIV polymorphisms and HLA. J. Exp. Med. 201:891–902.
15. **Kawashima Y, Pfafferott K, Frater J, Matthews P, Payne R, Addo M, Gatanaga H, Fujiwara M, Hachiya A, Koizumi H, Kuse N, Oka S, Duda A, Prendergast A, Crawford H, Leslie A, Brumme Z, Brumme C, Allen T, Brander C, Kaslow R, Tang J, Hunter E, Allen S, Mulenga J, Branch S, Roach T, John M, Mallal S, Ogwu A, Shapiro R, Prado JG, Fidler S, Weber J, Pybus OG, Klenerman P, Ndung'u T, Phillips R, Heckerman D, Harrigan PR, Walker BD, Takiguchi M, Goulder P.** 2009. Adaptation of HIV-1 to human leukocyte antigen class I. Nature 458:641–645.
16. **Avila-Rios S, Ormsby CE, Carlson JM, Valenzuela-Ponce H, Blanco-Heredia J, Garrido-Rodriguez D, Garcia-Morales C, Heckerman D, Brumme ZL, Mallal S, John M, Espinosa E, Reyes-Teran G.** 2009. Unique features of HLA-mediated HIV evolution in a Mexican cohort: a comparative study. Retrovirology 6:72. doi:10.1186/1742-4690-6-72.
17. **Boutwell CL, Essex M.** 2007. Identification of HLA class I-associated amino acid polymorphisms in the HIV-1C proteome. AIDS Res. Hum. Retroviruses 23:165–174.
18. **Brumme ZL, Brumme CJ, Heckerman D, Korber BT, Daniels M, Carlson J, Kadie C, Bhattacharya T, Chui C, Szinger J, Mo T, Hogg RS, Montaner JS, Frahm N, Brander C, Walker BD, Harrigan PR.** 2007. Evidence of differential HLA class I-mediated viral evolution in functional and accessory/regulatory genes of HIV-1. PLoS Pathog. 3:e94. doi:10.1371/journal.ppat.0030094.
19. **Carlson JM, Listgarten J, Pfeifer N, Tan V, Kadie C, Walker BD, Ndung'u T, Shapiro R, Frater J, Brumme ZL, Goulder PJ, Heckerman D.** 2012. Widespread impact of HLA restriction on immune control and escape pathways of HIV-1. J. Virol. 86:5230–5243.
20. **Carlson JM, Brumme ZL, Rousseau CM, Brumme CJ, Matthews P, Kadie C, Mullins JI, Walker BD, Harrigan PR, Goulder PJ, Heckerman D.** 2008. Phylogenetic dependency networks: inferring patterns of CTL escape and codon covariation in HIV-1 Gag. PLoS Comput. Biol. 4:e1000225. doi:10.1371/journal.pcbi.1000225.
21. **Rousseau CM, Daniels MG, Carlson JM, Kadie C, Crawford H, Pren-**

dergast A, Matthews P, Payne R, Rolland M, Raugi DN, Maust BS, Learn GH, Nickle DC, Coovadia H, Ndung'u T, Frahm N, Brander C, Walker BD, Goulder PJ, Bhattacharya T, Heckerman DE, Korber BT, Mullins JI. 2008. HLA class I-driven evolution of human immunodeficiency virus type 1 subtype C proteome: immune escape and viral load. J. Virol. 82:6434–6446.

22. Crawford H, Lumm W, Leslie A, Schaefer M, Boeras D, Prado JG, Tang J, Farmer P, Ndung'u T, Lakhi S, Gilmour J, Goepfert P, Walker BD, Kaslow R, Mulenga J, Allen S, Goulder PJ, Hunter E. 2009. Evolution of HLA-B*5703 HIV-1 escape mutations in HLA-B*5703-positive individuals and their transmission recipients. J. Exp. Med. 206:909–921.
23. Honeyborne I, Prendergast A, Pereyra F, Leslie A, Crawford H, Payne R, Reddy S, Bishop K, Moodley E, Nair K, van der Stok M, McCarthy N, Rousseau CM, Addo M, Mullins JI, Brander C, Kiepiela P, Walker BD, Goulder PJ. 2007. Control of human immunodeficiency virus type 1 is associated with HLA-B*13 and targeting of multiple gag-specific $CD8^+$ T-cell epitopes. J. Virol. 81:3667–3672.
24. Naruto T, Murakoshi H, Chikata T, Koyanagi M, Kawashima Y, Gatanaga H, Oka S, Takiguchi M. 2011. Selection of HLA-B57-associated Gag A146P mutant by HLA-B*48:01-restricted Gag140-147-specific CTLs in chronically HIV-1-infected Japanese. Microbes Infect. 13:766–770.
25. Goulder PJ, Bunce M, Krausa P, McIntyre K, Crowley S, Morgan B, Edwards A, Giangrande P, Phillips RE, McMichael AJ. 1996. Novel, cross-restricted, conserved, and immunodominant cytotoxic T lymphocyte epitopes in slow progressors in HIV type 1 infection. AIDS Res. Hum. Retroviruses 12:1691–1698.
26. Leslie AJ, Pfafferott KJ, Chetty P, Draenert R, Addo MM, Feeney M, Tang Y, Holmes EC, Allen T, Prado JG, Altfeld M, Brander C, Dixon C, Ramduth D, Jeena P, Thomas SA, St John A, Roach TA, Kupfer B, Luzzi G, Edwards A, Taylor G, Lyall H, Tudor-Williams G, Novelli V, Martinez-Picado J, Kiepiela P, Walker BD, Goulder PJ. 2004. HIV evolution: CTL escape mutation and reversion after transmission. Nat. Med. 10:282–289.
27. Miura T, Brockman MA, Schneidewind A, Lobritz M, Pereyra F, Rathod A, Block BL, Brumme ZL, Brumme CJ, Baker B, Rothchild AC, Li B, Trocha A, Cutrell E, Frahm N, Brander C, Toth I, Arts EJ, Allen TM, Walker BD. 2009. HLA-B57/B*5801 human immunodeficiency virus type 1 elite controllers select for rare gag variants associated with reduced viral replication capacity and strong cytotoxic T-lymphocyte recognition. J. Virol. 83:2743–2755.
28. Kawashima Y, Kuse N, Gatanaga H, Naruto T, Fujiwara M, Dohki S, Akahoshi T, Maenaka K, Goulder P, Oka S, Takiguchi M. 2010. Long-term control of HIV-1 in hemophiliacs carrying slow-progressing allele HLA-B*5101. J. Virol. 84:7151–7160.
29. Akari H, Arold S, Fukumori T, Okazaki T, Strebel K, Adachi A. 2000. Nef-induced major histocompatibility complex class I down-regulation is functionally dissociated from its virion incorporation, enhancement of viral infectivity, and CD4 down-regulation. J. Virol. 74:2907–2912.
30. Falk K, Rotzschke O, Takiguchi M, Gnau V, Stevanovic S, Jung G, Rammensee HG. 1995. Peptide motifs of HLA-B51, -B52 and -B78 molecules, and implications for Behcet's disease. Int. Immunol. 7:223–228.
31. Tomiyama H, Fujiwara M, Oka S, Takiguchi M. 2005. Cutting edge: epitope-dependent effect of Nef-mediated HLA class I down-regulation on ability of HIV-1-specific CTLs to suppress HIV-1 replication. J. Immunol. 174:36–40.
32. Tomiyama H, Akari H, Adachi A, Takiguchi M. 2002. Different effects of Nef-mediated HLA class I down-regulation on human immunodeficiency virus type 1-specific CD8(+) T-cell cytolytic activity and cytokine production. J. Virol. 76:7535–7543.
33. Takamiya Y, Schonbach C, Nokihara K, Yamaguchi M, Ferrone S, Kano K, Egawa K, Takiguchi M. 1994. HLA-B*3501-peptide interactions: role of anchor residues of peptides in their binding to HLA-B*3501 molecules. Int. Immunol. 6:255–261.
34. Huang KH, Goedhals D, Carlson JM, Brockman MA, Mishra S, Brumme ZL, Hickling S, Tang CS, Miura T, Seebregts C, Heckerman D, Ndung'u T, Walker B, Klenerman P, Steyn D, Goulder P, Phillips R, Bloemfontein-Oxford Collaborative Group, van Vuuren C, Frater J. 2011. Progression to AIDS in South Africa is associated with both reverting and compensatory viral mutations. PLoS One 6:e19018. doi:10.1371/journal.pone.0019018.
35. Altman JD, Moss PA, Goulder PJ, Barouch DH, McHeyzer-Williams MG, Bell JI, McMichael AJ, Davis MM. 1996. Phenotypic analysis of antigen-specific T lymphocytes. Science 274:94–96.
36. Kabsch W. 2010. XDS. Acta Crystallogr. D Biol. Crystallogr. 66(Pt 2):125–132.
37. Evans PR. 1993. Proceedings of the CCP4 Study Weekend on Data Collection & Processing. Daresbury Laboratory, Warrington, United Kingdom.
38. Matthews BW. 1968. Solvent content of protein crystals. J. Mol. Biol. 33:491–497.
39. Vagin A, Teplyakov A. 1997. MOLREP: an automated program for molecular replacement. J. Appl. Crystallogr. 30:1022–1025.
40. Murshudov GN, Vagin AA, Dodson EJ. 1997. Refinement of macromolecular structures by the maximum-likelihood method. Acta Crystallogr. D Biol. Crystallogr. 53:240–255.
41. Adams PD, Afonine PV, Bunkoczi G, Chen VB, Davis IW, Echols N, Headd JJ, Hung LW, Kapral GJ, Grosse-Kunstleve RW, McCoy AJ, Moriarty NW, Oeffner R, Read RJ, Richardson DC, Richardson JS, Terwilliger TC, Zwart PH. 2010. PHENIX: a comprehensive Python-based system for macromolecular structure solution. Acta Crystallogr. D Biol. Crystallogr. 66:213–221.
42. Laskowski RA, MacArthur MW, Moss DS, Thornton JM. 1993. PROCHECK: a program to check the stereochemical quality of protein structures. J. Appl. Crystallogr. 26:283–291.
43. Emsley P, Lohkamp B, Scott WG, Cowtan K. 2010. Features and development of Coot. Acta Crystallogr. D Biol. Crystallogr. 66:486–501.
44. Sakaguchi T, Ibe M, Miwa K, Yokota S, Tanaka K, Schonbach C, Takiguchi M. 1997. Predominant role of N-terminal residue of nonamer peptides in their binding to HLA-B* 5101 molecules. Immunogenetics 46:245–248.
45. Maenaka K, Maenaka T, Tomiyama H, Takiguchi M, Stuart DI, Jones EY. 2000. Nonstandard peptide binding revealed by crystal structures of HLA-B*5101 complexed with HIV immunodominant epitopes. J. Immunol. 165:3260–3267.
46. Sakaguchi T, Ibe M, Miwa K, Kaneko Y, Yokota S, Tanaka K, Takiguchi M. 1997. Binding of 8-mer to 11-mer peptides carrying the anchor residues to slow assembling HLA class I molecules (HLA-B*5101). Immunogenetics 45:259–265.
47. Hiraiwa M, Yamamoto J, Matsumoto K, Karaki S, Nagao T, Kano K, Takiguchi M. 1991. T cell can recognize the allospecificities formed by the substitution of amino acids associated with HLA-Bw4/Bw6 public epitopes. Hum. Immunol. 32:41–45.
48. Yamamoto J, Hiraiwa M, Hayashi H, Tanabe M, Kano K, Takiguchi M. 1991. Two amino acid substitutions at residues 63 and 67 between HLA-B51 and HLA-Bw52 form multiple epitopes recognized by allogeneic T cells. Immunogenetics 33:286–289.
49. Tomiyama H, Sakaguchi T, Miwa K, Oka S, Iwamoto A, Kaneko Y, Takiguchi M. 1999. Identification of multiple HIV-1 CTL epitopes presented by HLA-B*5101 molecules. Hum. Immunol. 60:177–186.
50. Zhang Y, Peng Y, Yan H, Xu K, Saito M, Wu H, Chen X, Ranasinghe S, Kuse N, Powell T, Zhao Y, Li W, Zhang X, Feng X, Li N, Leligdowicz A, Xu X, John M, Takiguchi M, McMichael A, Rowland-Jones S, Dong T. 2011. Multilayered defense in HLA-B51-associated HIV control. J. Immunol. 187:684–691.

Biochemical and Biophysical Research Communications 430 (2013) 592–597

Contents lists available at SciVerse ScienceDirect

Biochemical and Biophysical Research Communications

journal homepage: www.elsevier.com/locate/ybbrc

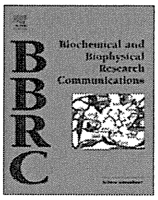

PML tumor suppressor protein is required for HCV production

Misao Kuroki[a,b,c], Yasuo Ariumi[a,c,*], Makoto Hijikata[d], Masanori Ikeda[a], Hiromichi Dansako[a], Takaji Wakita[e], Kunitada Shimotohno[f], Nobuyuki Kato[a]

[a] *Department of Tumor Virology, Okayama University Graduate School of Medicine, Dentistry, and Pharmaceutical Sciences, 2-5-1, Shikata-cho, Okayama 700-8558, Japan*
[b] *Research Fellow of the Japan Society for the Promotion of Science*
[c] *Center for AIDS Research, Kumamoto University, Kumamoto 860-0811, Japan*
[d] *Department of Viral Oncology, Institute for Virus Research, Kyoto University, Kyoto 606-8507, Japan*
[e] *Department of Virology II, National Institute of Infectious Diseases, Tokyo 162-8640, Japan*
[f] *Research Center for Hepatitis and Immunology, National Center for Global Health and Medicine, Ichikawa, Chiba 272-8516, Japan*

ARTICLE INFO

Article history:
Received 8 November 2012
Available online 5 December 2012

Keywords:
Hepatitis C virus
PML
INI1
DDX5
Tumor suppressor
Lipid droplet

ABSTRACT

PML tumor suppressor protein, which forms discrete nuclear structures termed PML-nuclear bodies, has been associated with several cellular functions, including cell proliferation, apoptosis and antiviral defense. Recently, it was reported that the HCV core protein colocalizes with PML in PML-NBs and abrogates the PML function through interaction with PML. However, role(s) of PML in HCV life cycle is unknown. To test whether or not PML affects HCV life cycle, we examined the level of secreted HCV core and the infectivity of HCV in the culture supernatants as well as the level of HCV RNA in HuH-7-derived RSc cells, in which HCV-JFH1 can infect and efficiently replicate, stably expressing short hairpin RNA targeted to PML. In this context, the level of secreted HCV core and the infectivity in the supernatants from PML knockdown cells was remarkably reduced, whereas the level of HCV RNA in the PML knockdown cells was not significantly affected in spite of very effective knockdown of PML. In fact, we showed that PML is unrelated to HCV RNA replication using the subgenomic HCV-JFH1 replicon RNA, JRN/3-5B. Furthermore, the infectivity of HCV-like particle in the culture supernatants was significantly reduced in PML knockdown JRN/3-5B cells expressing core to NS2 coding region of HCV-JFH1 genome using the *trans*-packaging system. Finally, we also demonstrated that INI1 and DDX5, the PML-related proteins, are involved in HCV production. Taken together, these findings suggest that PML is required for HCV production.

1. Introduction

Hepatitis C virus (HCV) is the causative agent of chronic hepatitis, which progresses to liver cirrhosis and hepatocellular carcinoma. HCV is an enveloped virus with a positive single-stranded 9.6 kb RNA genome, which encodes a large polyprotein precursor of approximately 3000 amino acid residues. This polyprotein is cleaved by a combination of the host and viral proteases into at least 10 proteins in the following order: core, envelope 1 (E1), E2, p7, non-structural 2 (NS2), NS3, NS4A, NS4B, NS5A, and NS5B [1,2]. HCV core protein forms a viral capsid and is essential for infectious virion production. The core protein is targeted to lipid droplets. Recently, lipid droplets have been found to be involved in an important cytoplasmic organelle for HCV production [3].

In addition, HCV core has been reported to facilitate cellular transformation as well as development of hepatocellular carcinoma in HCV core-transgenic mice [4]. Interactions of core with tumor suppressor proteins such as p53 and DDX3 may lead to enhanced cellular proliferation [4]. Indeed, HCV core interacts with promyelocytic leukemia (PML) protein and inhibits the PML tumor suppressor pathway through interfering with the PML-mediated apoptosis-inducing function [5]. PML forms discrete nuclear structures termed PML-nuclear bodies (PML-NBs) and associates with several cellular functions, including cell proliferation, apoptosis and antiviral defense [6,7]. In acute promyelocytic leukemia (APL) patient, the PML gene is fused with the retinoic acid receptor-α (RARα) gene, thus resulting in expression of an oncogenic PML-RARα fusion protein [6,7]. Conversely, treatment of APL patient with arsenic trioxide leads to reformation of PML-NBs and results in disease remission [6,7], indicating that PML is a target of arsenic trioxide. Interestingly, we have recently demonstrated that arsenic trioxide strongly inhibited HCV infection and HCV RNA replication without cell toxicity [8]. However, the role of PML in HCV life cycle yet remains unclear. To investigate the possible involvement of PML in HCV life cycle, we examined the accumulation of HCV RNA as well as the release of HCV core into culture

---

[*] Corresponding author at: Center for AIDS Research, Kumamoto University, 2-2-1, Honjo, Kumamoto 860-0811, Japan. Fax: +81 96 373 6834.
E-mail address: ariumi@kumamoto-u.ac.jp (Y. Ariumi).

0006-291X/$ - see front matter Crown Copyright © 2012 Published by Elsevier Inc. All rights reserved.
http://dx.doi.org/10.1016/j.bbrc.2012.11.108

supernatants from cells rendered defective for PML by RNA interference. The results provide evidence that PML is required for HCV production.

2. Materials and methods

2.1. Cell culture

293FT cells were cultured in Dulbecco's modified Eagle's medium (DMEM; Invitrogen, Carlsbad, CA, USA) supplemented with 10% fetal bovine serum (FBS). The three HuH-7-derived cell lines: RSc cured cells that cell culture-generated HCV-JFH1 (JFH1 strain of genotype 2a) [9] could infect and effectively replicate [10–13], OR6c cells is cured cells of OR6 cells harboring the genome-length HCV-O RNA with luciferase as a reporter [14] or OR6c JRN/3-5B cells harboring the subgenome HCV-JFH1 RNA with luciferase as a reporter were cultured in DMEM with 10% FBS as described previously [13].

2.2. RNA interference

Oligonucleotides with the following sense and antisense sequences were used for the cloning of short hairpin RNA (shRNA)-encoding sequences targeted to DDX5 in a lentiviral vector: 5′-GATCCCCCTCTAATGTGGAGTGCGACTTCAAGAGAGTCGCACTCCACATTAGAGTTTTTGGAAA-3′ (sense), 5′-AGCTTTTCCAAAAACTCTAATGTGGAGTGCGACTCTCTTGAAGTCGCACTCCACATTAGAGGGG-3′ (antisense). The oligonucleotides above were annealed and subcloned into the *Bgl*II-*Hind*III site, downstream from an RNA polymerase III promoter of pSUPER [15], to generate pSUPER-DDX5i. To construct pLV-DDX5i, the *Bam*HI-*Sal*I fragments of the pSUPER-DDX5i were subcloned into the *Bam*HI-*Sal*I site of pRDI292, an HIV-1-derived self-inactivating lentiviral vector containing a puromycin resistance marker allowing for the selection of transduced cells [16]. We previously described pLV-PMLi [8] and pLV-INI1i [17], respectively.

2.3. Lentiviral vector production

The vesicular stomatitis virus (VSV)-G-pseudotyped HIV-1-based vector system has been described previously [18,19]. The lentiviral vector particles were produced by transient transfection of the second-generation packaging construct pCMV-ΔR8.91 [18,19] and the VSV-G-envelope-expressing plasmid pMDG2 as well as pLV-PMLi into 293FT cells with FuGene6 (Roche Diagnostics, Mannheim, Germany).

2.4. HCV infection experiments

The supernatants was collected from cell culture-generated HCV-JFH1-infected RSc cells at 5 days post-infection and stored at −80 °C after filtering through a 0.45 μm filter (Kurabo, Osaka, Japan) until use. For infection experiments with HCV-JFH1 virus or J6/JFH1 [20], RSc cells (5×10^4 cells/well) were plated onto 6-well plates and cultured for 24 h (hrs). We then infected the cells at a multiplicity of infection (MOI) of 0.05. The culture supernatants were collected at the indicated time post-infection and the levels of the core protein were determined by enzyme-linked immunosorbent assay (Mitsubishi Kagaku Bio-Clinical Laboratories, Tokyo, Japan). Total RNA was isolated from the infected cellular lysates using RNeasy mini kit (Qiagen, Hilden, Germany) for quantitative RT-PCR analysis of intracellular HCV RNA. The infectivity of HCV-JFH1 in the culture supernatants was determined by a focus-forming assay at 48 h post-infection.

2.5. Quantitative RT-PCR analysis

The quantitative RT-PCR analysis for HCV RNA was performed by real-time LightCycler PCR (Roche) as described previously [14]. We used the following forward and reverse primer sets for the real-time LightCycler PCR: PML, 5′-GAGGAGTTCCAGTTTCTGCG-3′ (forward), 5′-GCGCCTGGCAGATGGGGCAC-3′ (reverse); DDX5, 5′-ATGTCGGGTTATTCGAGTGA-3′ (forward), 5′-TTTCTCCCCAGGGTTTCCAA-3′ (reverse); INI1, 5′-ATGATGATGATGGCGCTGAG-3′ (forward), 5′-TCGGAACATACGGAGGTAGT-3′ (reverse); β-actin, 5′-TGACGGGGTCACCCACACTG-3′ (forward), 5′-AAGCTGTAGCCGCGCTCGGT-3′ (reverse); and HCV-JFH1, 5′-AGAGCCATAGTGGTCTGCGG-3′ (forward), 5′-CTTTCGCAACCCAACGCTAC-3′ (reverse).

2.6. Western blot analysis

Cells were lysed in buffer containing 50 mM Tris–HCl (pH 8.0), 150 mM NaCl, 4 mM EDTA, 1% Nonidet P-40, 0.1% sodium dodecyl sulfate (SDS), 1 mM dithiothreitol and 1 mM phenylmethylsulfonyl fluoride. Supernatants from these lysates were subjected to SDS–polyacrylamide gel electrophoresis, followed by immunoblot analysis using anti-HCV core (CP-9 and CP-11; Institute of Immunology, Tokyo, Japan) or anti-β-actin antibody (Sigma).

2.7. WST-1 assay

RSc or OR6c JRN/3-5B cells (1×10^3 cells/well) were plated onto 96-well plates and cultured. The cells were subjected to the WST-1 cell proliferation assay (Takara Bio, Otsu, Japan) according to the manufacturer's protocol. The absorbance was read using a microplate reader at 440 nm with a reference wavelength of 690 nm.

2.8. Renilla luciferase (RL) assay

OR6c JRN/3-5B cells (1.5×10^4 cells/well) were plated onto 24-well plates and cultured for 72 h, then, subjected to the RL assay according to the manufacturer's instructions (Promega, Madison, WI, USA). A lumat LB9507 luminometer (Berthold, Bad Wildbad, Germany) was used to detect RL activity.

2.9. RNA synthesis and transfection

Plasmid pJRN/3-5B was linearized by digestion with *Xba*I and was used for RNA synthesis with T7 MEGAscript (Ambion) as previously described [13]. *In vitro* transcribed RNA was transfected into OR6c cells by electroporation as described previously [14].

2.10. Immunofluorescence and confocal microscopic analysis

Cells were fixed in 3.6% formaldehyde in phosphate-buffered saline (PBS), permeabilized in 0.1% Nonidet P-40 in PBS at room temperature, and incubated with anti-PML antibody (PM001, MBL) and anti-HCV core at a 1:300 dilution in PBS containing 3% bovine serum albumin (BSA) at 37 °C for 30 min. They were then stained with anti-Cy3-conjugated anti-mouse antibody (Jackson ImmunoResearch, West Grove, PA) or Alexa Fluor 647-conjugated anti-rabbit antibody (Molecular Probes, Invitrogen) at a 1:300 dilution in PBS containing BSA at 37 °C for 30 min. Lipid droplets and nuclei were stained with BODIPY 493/503 (Molecular Probes, Invitrogen) and DAPI (4′, 6′-diamidino-2-phenylindole), respectively. Following extensive washing in PBS, the cells were mounted on slides using a mounting media of SlowFade Gold antifade reagent (Invitrogen) added to reduce fading. Samples were viewed under a confocal laser-scanning microscope (FV1000; Olympus, Tokyo, Japan).